NASA TECHNICAL NOTE

NASA TN D-6880

DIGITAL-COMPUTER NORMAL-SHOCK-POSITION AND RESTART CONTROL OF A MACH 2.5 AXISYMMETRIC MIXED-COMPRESSION INLET

by George H. Neiner, Gary L. Cole, and Dale J. Arpasi

Lewis Research Center
Cleveland, Ohio 44135

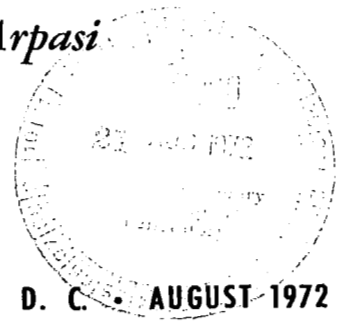

NATIONAL AERONAUTICS AND SPACE ADMINISTRATION • WASHINGTON, D. C. • AUGUST 1972

1. Report No.	2. Government Accession No.	3. Recipient's Catalog No.
NASA TN D-6880		

4. Title and Subtitle	5. Report Date
DIGITAL-COMPUTER NORMAL-SHOCK-POSITION AND RESTART CONTROL OF A MACH 2.5 AXISYMMETRIC MIXED-COMPRESSION INLET	August 1972
	6. Performing Organization Code

7. Author(s)	8. Performing Organization Report No.
George H. Neiner, Gary L. Cole, and Dale J. Arpasi	E-6498
	10. Work Unit No. 764-74

9. Performing Organization Name and Address	11. Contract or Grant No.
Lewis Research Center National Aeronautics and Space Administration Cleveland, Ohio 44135	
	13. Type of Report and Period Covered: Technical Note

12. Sponsoring Agency Name and Address	14. Sponsoring Agency Code
National Aeronautics and Space Administration Washington, D.C. 20546	

15. Supplementary Notes

16. Abstract

Results are presented for an investigation successfully demonstrating digital computer control of a mixed-compression inlet. The inlet was terminated with a choked orifice at the compressor face station to dynamically simulate a turbojet engine. Inlet diffuser exit airflow disturbances were used. A digital version of a previously tested analog control system was used for both normal shock and restart control. Digital computer algorithms were derived using z-transform and finite difference methods. Using a sample rate of 1000 samples per second, the digital normal shock and restart controls essentially duplicated the inlet analog computer control results. At a sample rate of 100 samples per second, the control system performed adequately but was less stable.

17. Key Words (Suggested by Author(s))
Automatic control, Supersonic inlets, Intake system, Supersonic inlet control, Normal shock control, Restart control, Digital computer control, Digital computer control of supersonic inlet

18. Distribution Statement
Unclassified - unlimited

19. Security Classif. (of this report)	20. Security Classif. (of this page)	21. No. of Pages	22. Price*
Unclassified	Unclassified	50	$3.00

* For sale by the National Technical Information Service, Springfield, Virginia 22151

CONTENTS

DIGITAL-COMPUTER NORMAL-SHOCK-POSITION AND RESTART CONTROL OF A MACH 2.5 AXISYMMETRIC MIXED-COMPRESSION INLET

by George H. Neiner, Gary L. Cole, and Dale J. Arpasi

Lewis Research Center

SUMMARY

Results are presented for an investigation successfully demonstrating on-line digital computer control of a supersonic inlet. A digital version of a previously tested analog computer normal shock and restart control system was used. Digital computer algorithms were derived using z-transform and finite difference methods. An analog computer inlet simulation was used to debug the digital computer controller algorithms and to predict inlet normal shock position dynamics. Experimental results show that the digital computer control essentially duplicated the analog control when the digital computer sample rate was 1000 samples per second. At a sample rate of 100 samples per second the control system performed adequately, but was less stable. This sample rate was also used during frequency response tests to demonstrate problems that occur at disturbance frequencies which exceed half the sampling frequency (as predicted by sampled-data theory).

The normal shock controller used either a throat exit static pressure or the output of an electronic shock position sensor for feedback. The shock sensor logic was based on eight cowl wall static pressures and had a stepwise-continuous output proportional to shock position. Frequency response tests of the normal shock control gave about the same results regardless of which feedback signal was used.

The inlet was sized for a J-85 turbojet engine. It was terminated at the diffuser exit with a choked orifice to dynamically simulate a turbojet engine. The inlet contained six high response, overboard bypass doors. Three of the doors were for control, while the other three doors were used to produce airflow disturbances. The tests were conducted in the Lewis 10- by 10-Foot Supersonic Wind Tunnel.

INTRODUCTION

The control system for a supersonic mixed-compression inlet should regulate the position of the normal shock while the inlet is subjected to upstream and/or downstream airflow disturbances. The normal shock should be positioned just aft of the inlet's throat, causing the inlet to operate with high total pressure recovery and low distortion of the total pressure profile at the diffuser exit.

If the normal shock is allowed to move ahead of the inlet's throat, it will move abruptly to a position outside of the inlet. Such an inlet unstart results in sharply reduced pressure recovery and increased distortion. Thus, a second function of the inlet control system is to affect a restart sequence that will return the inlet to normal operation. Activity in the area of inlet control, using analog computation, at the Lewis Research Center has been reported in references 1 to 4. These types of control have also been investigated by others (refs. 5 and 6).

Present day pneumatic-hydromechanical controls can accomplish normal shock and restart control. However, because of the computational capabilities of the digital computer, it can more easily handle the nonlinearities of the propulsion system over its flight envelope. Also, the digital computer can take into account other factors such as the aircraft and the external environment which would be more difficult for the pneumatic-hydromechanical control.

Digital control does not come without some problems and limitations. Some of these problems are as follows:

(1) Sample rate requirements: To be consistent with sampled-data theory, the measured parameters must be sampled at a frequency at least twice the highest frequency contained in those parameters that significantly could affect the system. Failure to observe this fact results in high frequency data being missed and may cause low frequency oscillations in the closed-loop system or even system instability. A practical example of this will be demonstrated in the RESULTS AND DISCUSSION section. This requirement places a physical limit on the calculation rate of the digital computer in that it must be capable of completing the calculation of the digital control function within one sample period.

(2) Sampled data skew: If more than one parameter must be sampled to calculate the control function, and if the sampling hardware operates in a sequential manner, dynamic errors will be introduced into the control if the time between parameter samples is not small compared to their frequency content.

(3) Quantization error: The input data are quantized by the number of sample levels being used for the range of each variable. This will set the ultimate accuracy of the system.

(4) Round-off errors: Numerical values in the computer must be truncated to fit the computer's finite word size. This will also limit the accuracy of the system.

(5) Numerical stability: Finite word size also limits the accuracy to which the coefficients of the control law or algorithm can be set. This problem can have an effect on numerical stability. Thus, it is possible for the control algorithm to be stable in theory, yet be numerically unstable when inserted into the experimental system.

(6) Computer malfunction: The use of electronic computation, analog or digital, presents the possibility of issuance of erroneous commands. A sudden full-scale command could have disasterous consequences. An engine mounted computer presents an environmental tolerance reliability problem, while a centrally located one presents a signal transmission reliability problem.

However, current large-capacity, flight-worthy digital computers make the use of digital computation for propulsion system control a possibility.

The objective of this investigation was to demonstrate that these problems could be overcome and that it is possible to use a modern digital computer process controller for direct control of a mixed-compression inlet. During the program reported herein, only the sample rate problem was investigated. None of the other above listed problems were evident during the program or in the data that were taken, although computer malfunctions and reliability problems were not within the scope of this investigation.

Investigation of normal shock and restart controls was considered a logical first step in developing an all electronic digital computer propulsion system control. This is, because of all the various control systems on an aircraft, the normal shock and restart controls require the fastest computer sample rates.

The axisymmetric inlet was designed for Mach 2.5 and was sized for a J85-13 turbojet engine. The inlet was a mixed compression type with 60 percent of the supersonic area contraction occurring internally at the design Mach number. It was terminated in a choked orifice at the engine compressor face station. This was used to dynamically simulate a turbojet engine termination without the actual use of an engine. The open loop response of normal shock position to a downstream airflow disturbance exhibited significant amplitudes (above 0.4 of its steady-state value) to 140 hertz.

The digital computer used in this program was designed for doing real time calculations. The computer was a general purpose process computer with capabilities beyond those required for this program. It had a core capacity of 16 384 words of 16-bit length and operated with a memory cycle time of 0.75 microsecond. It had a 64-channel analog-to-digital input capability and had 26 independent digital-to-analog output channels.

Results are presented for both normal shock position controls and restart controls. The experimental setup and procedure is discussed first. This is followed by a discussion of the determination of the digital normal shock position controller. The performance of the normal shock control is then discussed followed by the performance of the restart control system. The tests were conducted in the 10- by 10-Foot Supersonic Wind Tunnel at Lewis Research Center.

APPARATUS AND PROCEDURE

The inlet used for the investigation was an axisymmetric mixed-compression type with 60 percent of the supersonic area contraction occurring internally at the design Mach number of 2.5. All tests were conducted at the following free stream conditions: Mach number, 2.5; total temperature, 315 K; total pressure, 8.95 newtons per square centimeter; specific heat ratio, 1.4; Reynolds number, 3.88×10^6 (based on the cowl lip diameter). The inlet was operated at zero angle of attack during all tests.

Inlet

Inlet description. - An isometric view of the NASA designed inlet is shown in figure 1. The inlet had a cowl lip diameter of 47.3 centimeters, corresponding to a capture flow area of 1760 square centimeters. The inlet design capture corrected airflow was 16.2 kilograms per second.

Porous throat bleed regions were located on both the cowl and centerbody surfaces

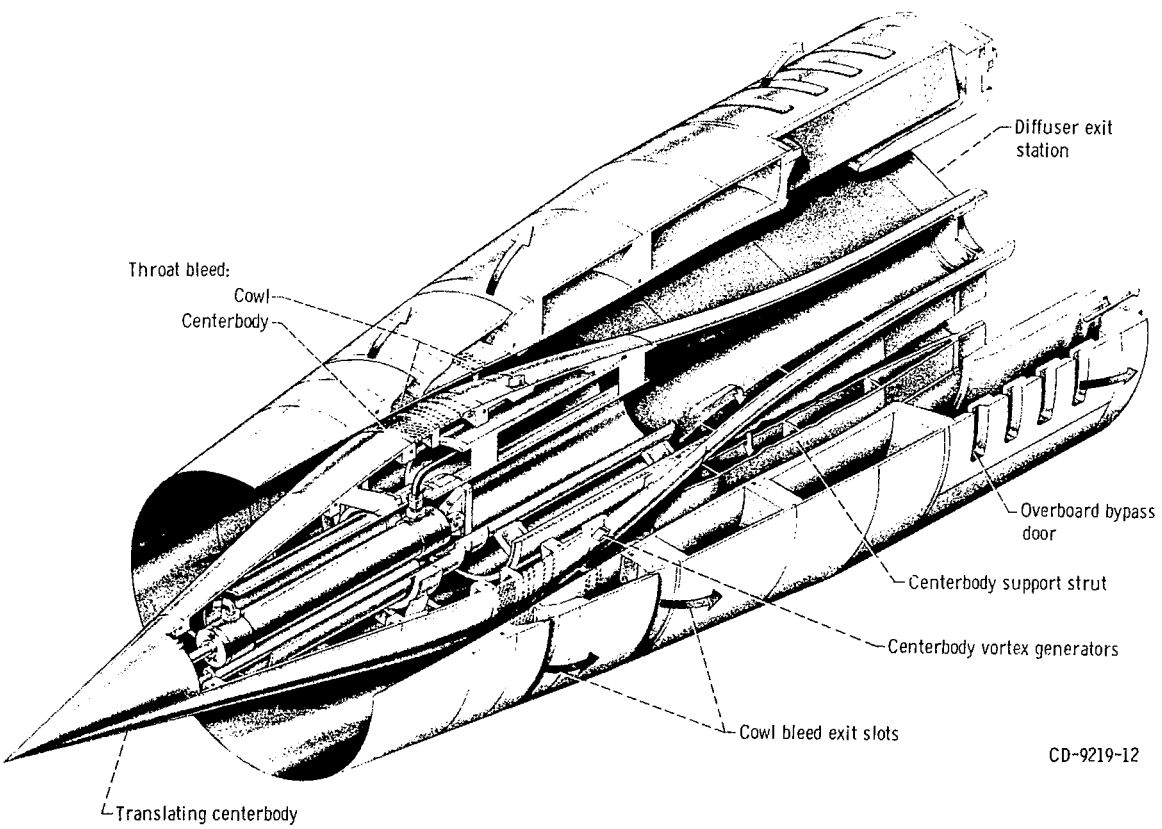

Figure 1. - Isometric view of inlet model.

(as shown in fig. 1). The bleed regions were used for boundary layer bleed and to improve the inlet's stability characteristics. Vortex generators were located on the centerbody to decrease distortion of the total pressure profile at the diffuser exit. Additional aerodynamic design details and steady-state performance characteristics of the inlet are given in references 7 and 8. The dynamic responses of various inlet internal pressures and of normal shock position to airflow disturbances are reported in reference 9.

Also shown in figure 1 is the inlet's translating centerbody which is hydraulically actuated and electronically controlled. The aft portion of the diffuser is compartmented by three struts which extend aft to the diffuser exit station. There are six bypass doors located symmetrically around the inlet just forward of the diffuser exit. They are hydraulically actuated and electronically controlled. The bypass doors are used to match inlet airflow to diffuser exit airflow requirements and are capable of bypassing approximately 88 percent of the design inlet capture airflow. The amplitude frequency response of each bypass door (for a peak-to-peak amplitude of 14 percent of full stroke) is flat within 0 to -3 decibels from 0 to 110 hertz. Additional details of the bypass door design can be found in references 8 and 10. Three symmetrically located bypass doors, driven in parallel, were used to provide sinusoidal disturbances in diffuser exit airflow. The remaining three bypass doors, also driven in parallel, were used as the manipulated variable for the various normal shock controllers.

Inlet termination. - Figure 2 shows the inlet installed in the wind tunnel. The inlet was terminated with a choked orifice plate located 146.5 centimeters downstream of the

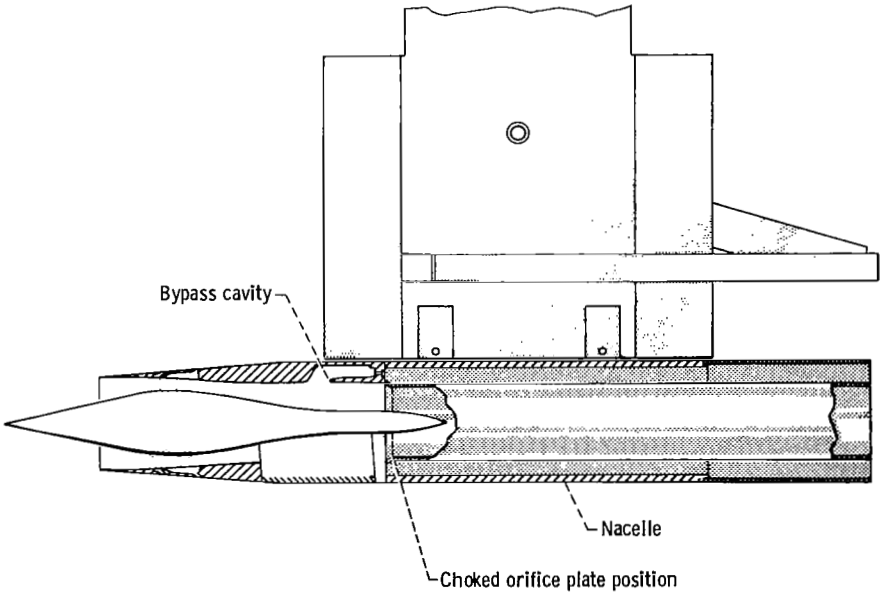

Figure 2. - Inlet installation showing choked orifice plate termination.

cowl lip (near the inlet diffuser exit). This termination was used because the dynamics of the inlet terminated by the choked orifice plate were found to be very similar to the dynamics of the inlet coupled to a turbojet engine (ref. 9). The geometrical flow area of the choked orifice plate was 598 square centimeters. Its flow coefficient was 0.985.

Inlet Instrumentation

Figures 3 and 4 indicate the location of pressure taps connected to dynamic strain-gage-type pressure transducers used in this investigation. In figure 4 static pressure measurements are indicated by solid circles, while total pressure measurements are denoted by open circles. The pressure tap locations are shown in centimeters from the cowl lip. The pressure transducers were close coupled to the pressure taps to enhance their dynamic response. The frequency response of each transducer and its coupled line was flat within 0 to +3 decibels to approximately 250 hertz.

The cowl lip static pressure P_{cl} and throat total pressure H_{th} were used with the restart control system to determine if the inlet was started or unstarted. (Symbols are defined in appendix A.) The eight throat static pressure signals were used as inputs to an electronic normal shock position sensor. This sensor was implemented on both a general purpose analog computer and on a digital computer. Both of these implementations are discussed in appendix B. The output produced by either implementation was a step-

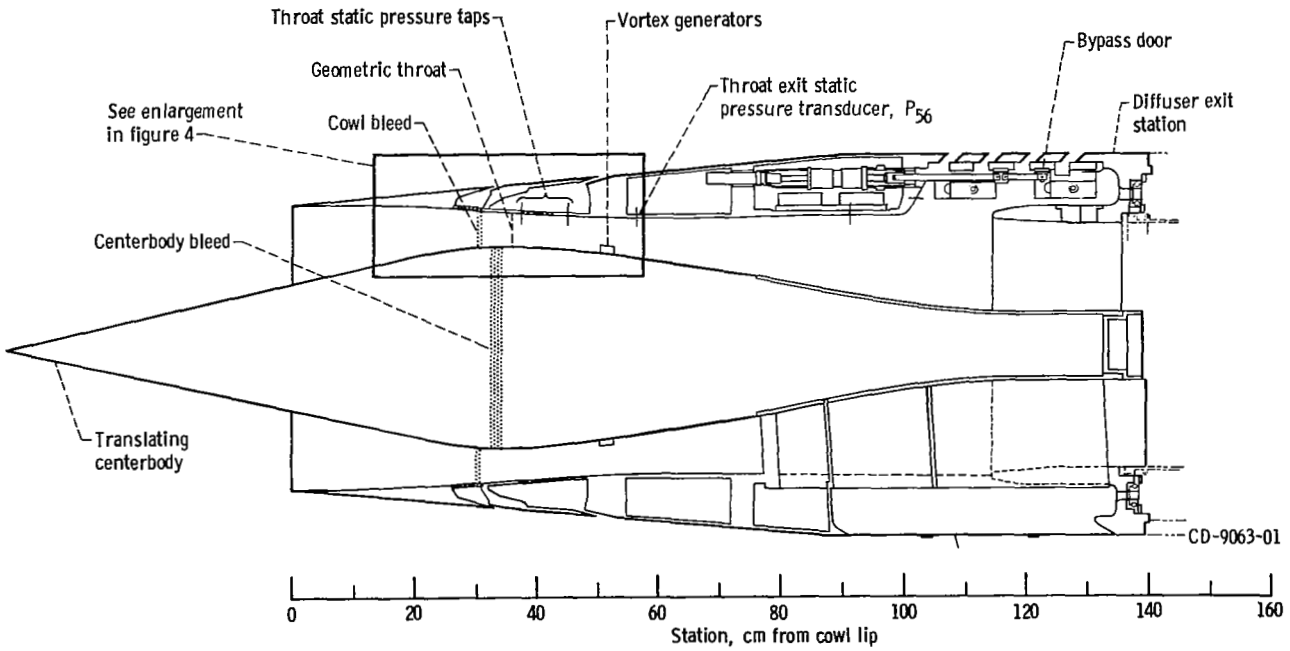

Figure 3. - Inlet details.

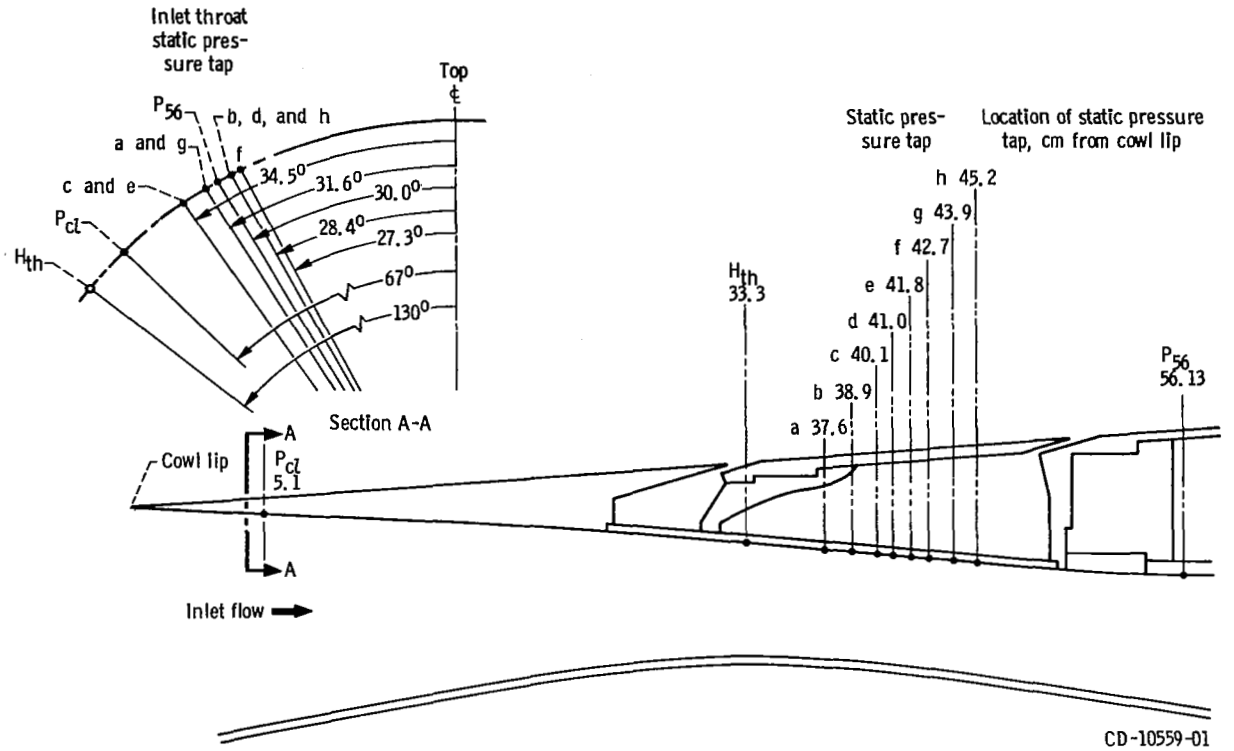

Figure 4. - Locations of inlet static pressure taps close coupled to dynamic pressure transducers used for normal shock and restart controls. (Pressure taps located in centimeters from the cowl lip.)

wise continuous signal proportional to the shock position. The various shock position controls tested used either the throat exit static pressure P_{56} or the stepwise continuous shock position signal as the feedback signal for control.

Controller Implementation

The normal shock position and restart controllers were implemented on both an analog and a digital computer, both computers were located in the wind tunnel control room. The analog computer was a desk-top-size 10-volt general purpose type. The digital computer was a commercially available high speed general purpose computer for real time control applications.

Figure 5 is a photograph of the complete digital computer setup. It is a general purpose control system designed for implementation of both inlet and engine controls. The system, shown in block diagram form in figure 6, consists of four major units.

(1) A digital computer with 16 384 words of memory, a read-restore memory cycle of 750 nanoseconds, and word length of 16 bits.

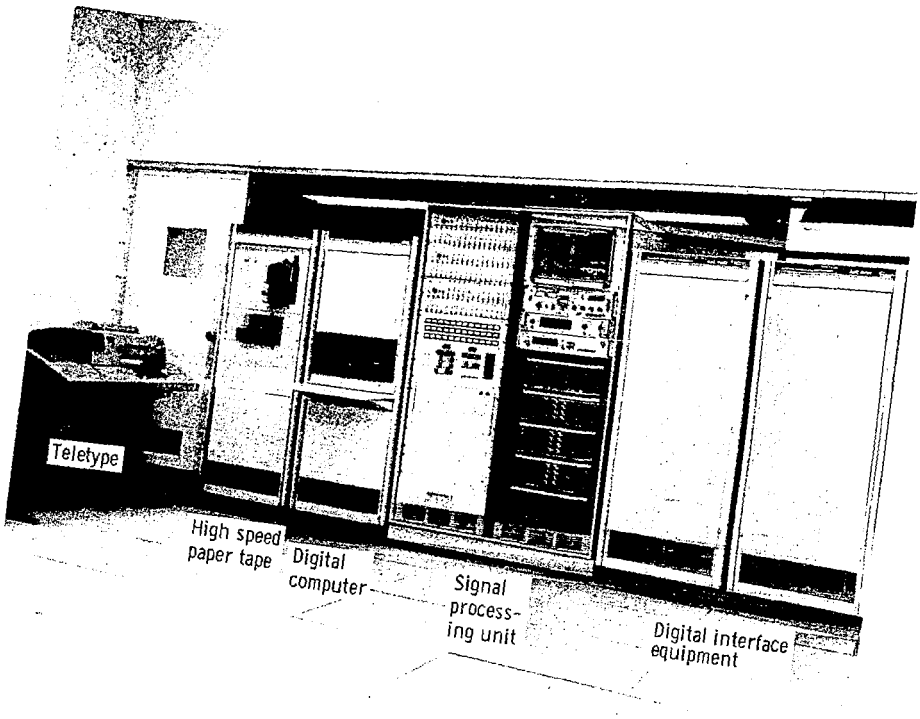

Figure 5. - Digital computer setup.

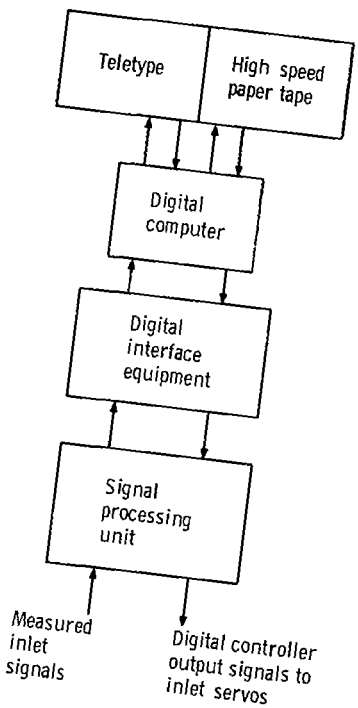

Figure 6. - Schematic of digital computer setup.

(2) A digital interface capable of converting both analog and frequency signals to computer compatible digital words and converting computer generated words to analog and logical outputs.

(3) A signal processing unit which provides signal conditioning and monitoring capability between the digital interface and the propulsion system to be controlled.

(4) Programming peripherals consisting of a high speed paper-tape reader and punch, and a teletype.

The capabilities of the system are given in table I and a comprehensive description is available in reference 11.

All inlet pressure measurements were passed through signal conditioners and isolation amplifiers to provide high level (-10 to +10 V) inputs to the digital interface unit. This unit consisted of a random access multiplexer, a sample and hold amplifier, and a 13-bit digitizer. The complete digitizing process from channel sample command to entry of the digitized measurement into computer memory requires approximately 50 microseconds. This process is automated through the use of a block data transfer unit which ties up the computer program execution for only one memory cycle per word transferred. Completion of the sampling process is conveyed to the computer by a priority interrupt from the block data transfer unit.

Digital commands are issued direct from the digital computer to the 13-bit digital-to-analog converters. These outputs are passed through isolation amplifiers in the control room to provide ground isolation of the digital system and then to the servoamplifiers driving the manipulated variables.

Test Procedure

The normal shock position controls used P_{56} or the stepwise continuous shock position sensor signal as feedback signals. These signals, after being operated on by either the analog or digital computer controller, were then used to manipulate the inlet bypass doors to control the normal shock. Three symmetrically spaced bypass doors were used for control, and the other three symmetrically spaced bypass doors were used to generate a downstream airflow disturbance. The disturbance bypass doors were oscillated sinusoidally at an amplitude sufficient to move the normal shock over the eight throat static pressure taps (fig. 4) at 1 hertz, while the control bypass doors remained fixed. The steady-state operating point of the normal shock was located near the middle of the eight throat statics.

For the dynamic tests, both magnitude and phase data for a few key signals were determined on-line using a commercial frequency response analyzer in the control room. These dynamic signals, as well as others, were recorded in analog form on magnetic

TABLE I. - DIGITAL SYSTEM CAPABILITIES

Digital computer	
Magnetic core memory size, words	16 384
Word length, bits plus parity	16
Memory cycle time, nsec	750
Add time, μsec	1.5
Multiply time, μsec	4.5
Divide time, μsec	8.25
Load time, μsec	1.5
Indirect addressing	Infinite
Indexing	Total memory
Priority interrupts	28 separate levels
Index registers	2
Interval timers	2
Analog acquisition unit	
Overall sample rate (maximum, kHz)	20
Resolution of digital data, bits	12 (plus sign)
Output code	Two's complement
Number of channels	64
Input range, V full scale	±10
Conversion time, μsec	38
Total error with calibration, percent	0.073
Analog output unit	
Total number of digital-to-analog conversion channels (DAC)	26
Resolution 13 bit DAC (10 channels), bits (12+1)	12 (plus sign)
Accuracy (13 bit) DAC, percent of full scale	±0.05
Resolution 12 bit DAC (16 channels), bits (11+1)	11 (plus sign)
Accuracy (12 bit DAC), percent of full scale	±0.1
Output voltage range, V full scale	±10
Slew rate, V/μsec	1
Priority interrupt processor	
Number of channels	10
Input voltage range, V	±10
Computer switching	Trigger on rise or fall
Comparator hysteresis, mV	Adjustable from 35 to 650
Comparator output, V	7

tape for reduction at a later time. Prior to each dynamic test, steady-state data were taken at the operating point and at each extreme point. These data gave the steady-state open-loop gains. After correcting the dynamic data to account for dynamics of the bypass doors, the data were plotted in the form of Bode plots, which show magnitude and phase shift as a function of frequency. The magnitude data were normalized by the steady-state open-loop gain.

The restart controls were programmed on both the analog and digital computers. A pulse-type disturbance from the three disturbance bypass doors produced the inlet unstart. The restart controls were evaluated by monitoring inlet internal pressure transients, as well as various other inlet signals throughout the unstart-restart cycle.

DEVELOPMENT OF DIGITAL CONTROLLER

Besides demonstrating the capabilities of a digital computer control system, it was desired to compare operation of the digital computer control with that of a continuous analog control. To accomplish this, it was necessary to have results from both digital and analog computer controllers, using the same control law. The inlet used in this investigation had been studied previously using various continuous controllers, implemented on an analog computer. Thus, it was desirous to use one of these previously studied analog controllers as the base line check for the digital computer controls work.

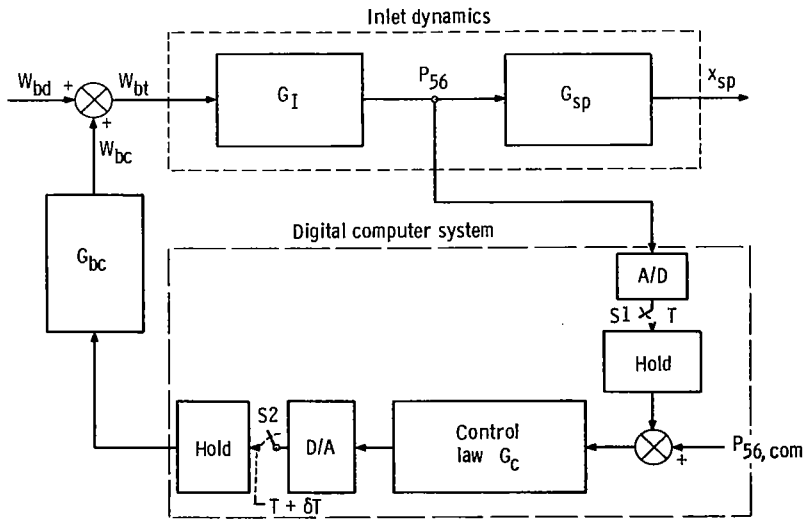

Figure 7. - Digital control system block diagram.

Control System Block Diagram Discussion

A block diagram of the digital control system is shown in figure 7. A downstream airflow disturbance W_{bd} is shown as the input to the system since the purpose of the control is to regulate shock position (or P_{56}) against such disturbances. The block G_I represents the inlet dynamics between bypass airflow and throat exit static pressure (P_{56}) and G_{sp} represents the dynamics between shock position and throat exit static pressure. The variable being controlled (P_{56} in the case of fig. 7) is sampled once every T seconds rather than being continuously fed to the controller as in the analog computer control case.

The control law or algorithm, programmed on the digital computer was the digital equivalent of a previously studied analog controller. The analog controller transfer function G_c was

$$G_c(s) = \frac{K_{c56}\left(\frac{s^2}{\omega_1^2} + \frac{2\rho s}{\omega_1} + 1\right)}{s\left(\frac{s}{\omega_2} + 1\right)} \qquad (1)$$

where $\omega_1 = 318$ radians per second, $\omega_2 = 316$ radians per second, and $\rho = 0.2$.

In figure 7 the digital computer system is followed by the block G_{bc} which represents the dynamics between the bypass door command voltage and the control bypass door airflow.

Determination of Digital Control Algorithm

The performance of a previously tested analog controller was to be used as the reference or baseline means of comparison for the performance of the digital controller. Thus, it was only necessary to obtain the digital controller equivalent (digital computer algorithm) of the analog controller transfer function. Two common methods for obtaining a computer algorithm were used. They were the z-transform method (refs. 12 and 13) and a finite difference approximation method. Both methods result in a computer algorithm of the general form

$$BPC(nT) = C_1ERR(nT) + C_2ERR(nT - T) + C_3ERR(nT - 2T) + C_4BPC(nT - T) + C_5BPC(nT - 2T) \qquad (2)$$

where ERR(nT) is a parameter error signal at the n^{th} sampling time and BPC(nT) is the bypass door command to be given at that instant.

The z-transform method is probably most common for arriving at the algorithm and also gives the most exact representation of the analog controller. On the other hand, the finite difference method is easier to apply and results in control equation coefficients (C_1, C_2, etc.) which are less complicated. Thus its control equation has the advantage of being computed more easily and quickly than that of the z-transform. This could be advantageous in an adaptive-type control where the coefficients would have to be calculated on-line. Computer algorithms arrived at by both the z-transform and finite difference methods were tested experimentally so that the performance and relative merits of the two methods could be compared with the results for analog computer control.

The z-Transform Method

Ideally the signal from a sampler is an impulse. The z-transform method is considered to be valid if the sampling duration or pulse width of the sampler is small when compared to the significant time constant of the system. This was felt to be satisfied by both the input and output samplers of this system which had sampling durations of approximately 9 microseconds and 1 microsecond, respectively. These times correspond to frequencies of about 10^5 radians per second (16 000 Hz) and 10^6 radians per second (160 000 Hz) which are well beyond the significant frequencies of this system.

The first step in determining the z-transform digital computer algorithm is to calculate a digital compensator equivalent to the analog compensator by taking the z-transform of the product of the analog compensator and a zero-order hold (ref. 12). That is,

$$G_c(z) = \mathscr{Z}[G_o(s)G_c(s)] \tag{3}$$

where s represents the Laplace variable, z the z-transform variable, $\mathscr{Z}$ the z-transform operator, and $G_o(s)$ and $G_c(s)$ are the transfer functions for a zero-order hold and for the analog compensator, respectively. The expressions for the transfer functions $G_o(s)$ and $G_c(s)$ (previously defined) are

$$G_o(s) = \frac{1 - e^{-Ts}}{s} \tag{4}$$

TABLE II. - GENERAL EXPRESSION FOR DIGITAL COMPUTER ALGORITHM COEFFICIENTS

[General form of algorithm: $BPC(nT) = C_1ERR(nT) + C_2ERR(nT - T) + C_3ERR(nT - 2T) + C_4BPC(nT - T) + C_5BPC(nT - 2T)$.]

z-transform coefficients

$$C_1 = K_{c56}\frac{\omega_2}{\omega_1^2}$$

$$C_2 = K_{c56}\left[T - \frac{2\omega_2}{\omega_1^2} + \frac{2\rho}{\omega_1}\left(1 - e^{-\omega_2 T}\right) + \frac{e^{-\omega_2 T} - 1}{\omega_2}\right]$$

$$C_3 = K_{c56}\left[\frac{\omega_2}{\omega_1^2} - e^{-\omega_2 T}T + \frac{2\rho}{\omega_1}\left(e^{-\omega_2 T} - 1\right) + \frac{\left(1 - e^{-\omega_2 T}\right)}{\omega_2}\right]$$

$$C_4 = 1 + e^{-\omega_2 T}$$

$$C_5 = -e^{-\omega_2 T}$$

Advanced z-transform coefficients

$$C_1 = K_{c56}\left[\omega_2\frac{e^{-\delta T\omega_2}}{\omega_1^2} + \delta T - \frac{2\rho}{\omega_1}\left(e^{-\delta T\omega_2} - 1\right) + \frac{\left(e^{-\delta T\omega_2} - 1\right)}{\omega_2}\right]$$

$$C_2 = K_{c56}\left[T - \delta T\left(1 + e^{-T\omega_2}\right) - 2\omega_2\frac{e^{-\delta T\omega_2}}{\omega_1^2} + \frac{2\rho}{\omega_1}\left(2e^{-\delta T\omega_2} - 1 - e^{-\omega_2 T}\right) + \frac{\left(e^{-\omega_2 T} - 2e^{-\delta T\omega_2} + 1\right)}{\omega_2}\right]$$

$$C_3 = K_{c56}\left[\frac{\omega_2}{\omega_1^2}e^{-\delta T\omega_2} - e^{-\omega_2 T}(1 - \delta)T + \frac{2\rho}{\omega_1}\left(e^{-\omega_2 T} - e^{-\delta T\omega_2}\right) + \frac{\left(e^{-\delta T\omega_2} - e^{-\omega_2 T}\right)}{\omega_2}\right]$$

$$C_4 = 1 + e^{-\omega_2 T}$$

$$C_5 = -e^{-\omega_2 T}$$

Backward finite difference coefficients

$$C_1 = \frac{K_{c56}\omega_2}{\omega_1^2(1 + \omega_2 T)}\left(1 + 2\rho T\omega_1 + \omega_1^2 T^2\right)$$

$$C_2 = \frac{-2K_{c56}\omega_2}{\omega_1^2(1 + \omega_2 T)}(1 + \rho\omega_1 T)$$

$$C_3 = \frac{K_{c56}\omega_2}{\omega_1^2(1 + \omega_2 T)}$$

$$C_4 = \frac{2 + \omega_2 T}{1 + \omega_2 T}$$

$$C_5 = \frac{-1}{1 + \omega_2 T}$$

Forward finite difference coefficients

$$C_1 = \frac{K_{c56}\omega_2}{\omega_1^2}$$

$$C_2 = \frac{-2K_{c56}\omega_2}{\omega_1^2}(1 - \rho\omega_1 T)$$

$$C_3 = \frac{K_{c56}\omega_2}{\omega_1^2}\left(1 + \omega_1^2 T^2 - 2\rho\omega_1 T\right)$$

$$C_4 = 2 - \omega_2 T$$

$$C_5 = -(1 - \omega_2 T)$$

$$G_c(s) = \frac{K_{c56}\left(\frac{s^2}{\omega_1^2} + \frac{2\rho s}{\omega_1} + 1\right)}{s\left(\frac{s}{\omega_2} + 1\right)} \tag{1}$$

When the operation of equation (3) is performed, the following digital compensator is obtained:

$$G_c(z) = \frac{C_1 z^2 + C_2 z + C_3}{z^2 - C_4 z - C_5} \tag{5}$$

where the C's depend on K_{c56}, ω_1, ω_2, ρ, T and are given in table II. Since $G_c(z)$ represents the transfer function between the compensator input (error in controlled variable) and the output (bypass command) at any sample instant nT, equation (5) can be expressed as

$$\frac{BPC(nT)}{ERR(nT)} = \frac{C_1 z^2 + C_2 z + C_3}{z^2 - C_4 z - C_5} \tag{6}$$

The digital computer algorithm is simply obtained from equation (6) by rearranging it as follows:

$$\left(z^2 - C_4 z - C_5\right)BPC(nT) = \left(C_1 z^2 + C_2 z + C_3\right)ERR(nT) \tag{7}$$

Multiplying by the inverse of the highest power of z gives

$$\left(1 - C_4 z^{-1} - C_5 z^{-2}\right)BPC(nT) = \left(C_1 + C_2 z^{-1} + C_3 z^{-2}\right)ERR(nT) \tag{8}$$

Since $z \equiv e^{sT}$ or $z^{-1} = e^{-sT}$, then $z^{-1}BPC(nT) = BPC(nT - T)$, $z^{-2}BPC(nT) = BPC(nT - 2T)$, and so forth. By making such substitutions and rearranging terms, equation (8) becomes the general form

$$BPC(nT) = C_1ERR(nT) + C_2ERR(nT - T) + C_3ERR(nT - 2T)$$

$$+ C_4BPC(nT - T) + C_5BPC(nT - 2T)$$

which is identical to equation (2).

Equation (2) is one which can be easily programmed on a digital computer. However, inspection of equation (2) reveals that a problem exists. Equation (2) states that the digital controller output (bypass door command) at any sample instant nT depends on the previous two outputs, BPC(nT - T) and BPC(nT - 2T), and the error at instant nT as well as the previous two errors, ERR(nT - T) and ERR(nT - 2T). The problem is that the computer must output a command at the same instant it is sampling the information upon which the output depends. This requires zero computation time by the computer. This problem arose because a compensator was chosen which had a numerator equal in order to its denominator. The problem does not exist when a compensator is chosen to have a denominator at least one order higher than the numerator. In that case the output at a given instant nT depends only on information from previous sample times. That was not done in this program because no analog compensator with a higher order denominator had been previously tested.

Since zero computation time is not possible, the output required at time nT will really be made after computation, at time nT + δT. This means that the output sampler is now not synchronous with the input sampler. This problem of nonsynchronous sampling can be compensated for by using the advanced z-transform. Reference 13 explains how this can be done analytically. The output of the compensator is first advanced in time by δT (where δT is the time by which the input and output samples are separated). This is accomplished in the Laplace (frequency) domain by multiplying by $e^{\delta Ts}$. The output sampler is then assumed to operate synchronously with the input sampler, but is followed by an equal dead time of δT. The sampler separation time δT is the time lapse from the end of the input sample hold to the beginning of the output sample and is found to be about 0.200 millisecond. Taking the advanced z-transform $\mathcal{Z}_a[G_o(s)G_c(s)]$ results in a compensator equivalent to the z-transform followed by the advance $e^{\delta Ts}$. The coefficients of the algorithm determined from the advanced z-transform digital compensator are listed in table II. As can be seen from the table, only the error term coefficients (C_1 to C_3) are changed from those of the z-transform and as expected those reduce to the z-transform coefficients when δ is zero. Actual values of the coefficients for the algorithms as determined by the z-transform and the advanced z-transform methods are given in table III. The constants are given for the specific case where K_{c56} = 30 volts per second per volt, ρ = 0.200, ω_1 = 318 radians per second, ω_2 = 316 radians per second, T = 0.00100 second, δ = 0.200. The coefficients were calculated off-line on a digital computer. However, there is no reason why the coefficients

TABLE III. - NUMERICAL VALUES OF DIGITAL COMPUTER ALGORITHM COEFFICIENTS AND PERCENT ERROR E_n OF COEFFICIENTS RELATIVE TO ADVANCED z-TRANSFORM COEFFICIENTS

[K_{c56} = 30 (V/sec)/V, ρ = 0.200, ω_1 = 318 rad/sec, ω_2 = 316 rad/sec, T = 0.00100 sec, δ = 0.200.]

Method	C_1	C_2	C_3	C_4	C_5
z-transform	0.0937	-0.173	0.0874	1.73	-0.729
Advanced z-transform	.0905	-.165	.0825	1.73	-.729
Backward difference	.0875	-.152	.0712	1.76	-.760
Forward difference	.0937	-.176	.0913	1.68	-.684
Method	$\lvert E_1 \rvert$	$\lvert E_2 \rvert$	$\lvert E_3 \rvert$	$\lvert E_4 \rvert$	$\lvert E_5 \rvert$
z-transform	3.5	4.9	5.9	0	0
Backward difference	3.3	7.9	14	1.7	4.3
Forward difference	3.5	6.7	11	2.9	6.2

could not be calculated on-line while the inlet was being controlled. They were also calculated for a particular δ, T, and K_{c56} and if δ, T, or K_{c56} is changed, new coefficients would have to be calculated.

The percent difference in the coefficients of the z-transform relative to the advanced z-transform coefficients are also given in table III. The greatest difference for the z-transform coefficients occurs in C_3 and is about 6 percent. Because of the small difference between the z-transform and advanced z-transform algorithms and the simpler programming required by the z-transform coefficients the z-transform equation instead of the advanced z-transform equation was selected for testing during the experimental program.

Finite Difference Methods

As indicated earlier, one advantage of the finite difference method over the z-transform is that the resulting algorithm coefficients are more easily computed. Also, the expressions for the algorithm coefficients are considerably simpler than those arrived at by the z-transform or advanced z-transform. Specifically, the exponential terms $e^{-\omega_2 T}$ and $e^{-\omega_2 \delta T}$ are eliminated. This eliminates the need for a table lookup or for a subroutine which can calculate such terms thereby reducing the computer's com-

putational requirements if coefficients are calculated on-line. Thus algorithms determined by finite difference methods were investigated and one was tested experimentally. Finite difference methods were considered, which approximated the derivatives by either the backward difference or the forward difference.

Backward difference approximation. - The backward difference approximations for the first and second derivatives of a variable y at any instant nT are

$$\dot{y}(nT) = \frac{y(nT) - y(nT - T)}{T} \tag{9}$$

$$\ddot{y}(nT) = \frac{y(nT) - 2y(nT - T) + y(nT - 2T)}{T^2} \tag{10}$$

As presented earlier, the analog compensator (eq. (1)) was

$$G_c(s) = \frac{BPC(s)}{ERR(s)} = \frac{K_{c56}\left(\frac{s^2}{\omega_1^2} + \frac{2\rho s}{\omega_1} + 1\right)}{s\left(\frac{s}{\omega_2} + 1\right)} \tag{1}$$

which can be rearranged as

$$\left(\frac{s^2}{\omega_2} + s\right) BPC(s) = K_{c56}\left(\frac{s^2}{\omega_1^2} + \frac{2\rho s}{\omega_1} + 1\right) ERR(s) \tag{11}$$

Multiplying by ω_2 and substituting $d^2/dt^2 = s^2$ and $d/dt = s$ gives

$$\ddot{BPC} + \omega_2 \dot{BPC} = K_{c56} \frac{\omega_2}{\omega_1^2} \ddot{ERR} + \frac{2K_{c56}\rho\omega_2}{\omega_1} \dot{ERR} + K_{c56}\omega_2 ERR \tag{12}$$

Substituting the approximations for the derivatives (eqs. (9) and (10)) into equation (12) reduces equation (12) to the general form given in equation (2) and is restated here

$$BPC(nT) = C_1ERR(nT) + C_2ERR(nT - T) + C_3ERR(nT - 2T)$$

$$+ C_4BPC(nT - T) + C_5BPC(nT - 2T) \qquad (2)$$

The general expressions for the coefficients are given in table II.

As was the case for the z-transform algorithm, the output BPC(nT) depends on the input ERR(nT), which requires zero computation time. The finite difference method can with considerable difficulty compensate for the displacement in time between the input and output samplers. However, this would defeat the purpose of using the simpler finite difference method. Also it may not be necessary to compensate for the time displacement if it is small enough. Experimental data to be shown later seem to verify this fact.

It can be seen from table II that the backward difference equation coefficients are much simpler than those derived by the z-transform or advanced z-transform method. Consequently, the computational effort required is much less. The actual values of the backward difference coefficients are also given in table III for the specific controller tested. It is seen that the coefficients are different from the advanced z-transform coefficients by as much as 14 percent. This backward difference algorithm was tested experimentally to determine what effect the differences in coefficients would have on controller performance.

Forward difference approximation. - The forward difference approximations for the first and second derivatives of a variable y at any instant nT are:

$$\dot{y}(nT) = \frac{y(nT + T) - y(nT)}{T} \qquad (13)$$

$$\ddot{y}(nT) = \frac{y(nT + 2T) - 2y(nT + T) + y(nT)}{T^2} \qquad (14)$$

Using these approximations for the derivatives and displacing the results backward in time by 2T again results in an algorithm of the general form as given in equation (2). As with the backward difference equation, this equation cannot be implemented exactly because the output depends on the term ERR(nT).

The general expressions for the coefficients are given in table II. It can be shown that, if the approximation $e^{-\omega_2 T} \approx 1 - \omega_2 T$ is substituted into the expressions for the z-transform coefficients they will reduce to the expressions arrived at by the forward difference method. Thus the forward difference effectively approximates $e^{-\omega_2 T}$ by the truncated series $1 - \omega_2 T$ (which of course is much easier to compute than $e^{-\omega_2 T}$).

This is not a good approximation, however, because $1 - \omega_2 T$ can change sign whereas $e^{-\omega_2 T}$ is always positive. This approximation can also result in controller instability. It can be shown that $1 - \omega_2 T$ is a pole (in the z-plane) of the digital compensator. Since poles outside of the unit circle $|z| = 1$ are unstable, it is seen that the controller will be unstable for $\omega_2 T < 0$ or $\omega_2 T > 2$. For the specific controller of interest ($\omega_2 = 316$), T is restricted to the range from 0 to 0.00633 second. Because it was desired to use the algorithms for sample periods as high as 0.010 second, this method was eliminated from consideration for experimental testing. Although they were not used, the coefficients and their errors are shown in table III for completeness.

Typical Sample Period for the Digital Computer Used

A typical sample period for the computer system used during the investigation is shown in figure 8. It shows the sequence of events that occur between the sampling of

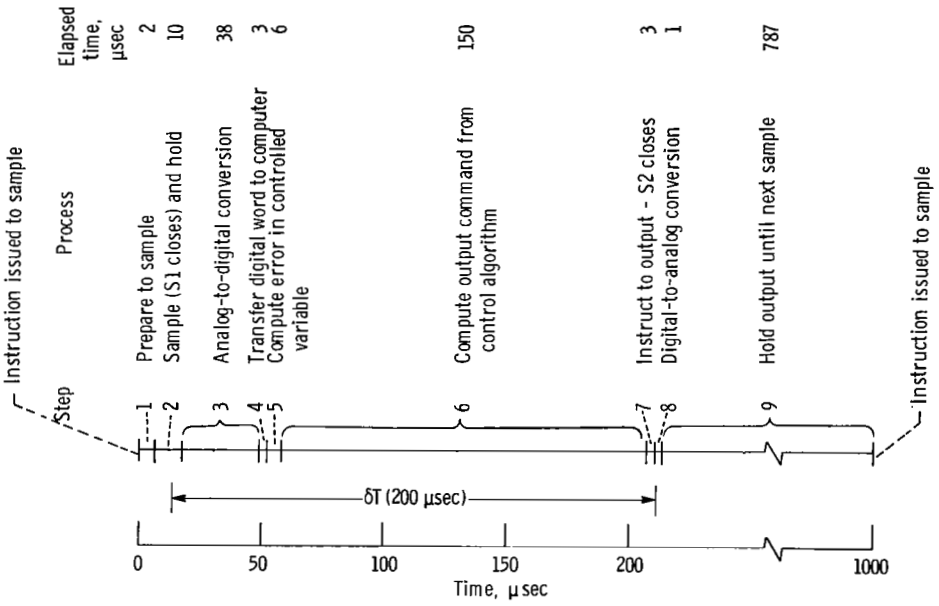

Figure 8. - Approximate digital computer operating times for typical 1-millisecond sample period T.

switch S1 in figure 7 and the output to the controlled system through switch S2. The numbers correspond to the following steps:

(1) The instruction is issued for a sample of the controller variable to be made and 2 microseconds later the analog signal is ready to be recorded.

(2) The sample-and-hold process occurs over a period of 10 microseconds.

(3) The sample is then digitized which requires 38 microseconds.

(4) The sampled digital data is then transferred to the computer in 3 microseconds.

(5) The error in the controlled variable is calculated by the computer, requiring approximately 6 microseconds.

(6) The command to the manipulated variable (the bypass doors) is calculated from the control law or algorithm. This required 150 microseconds.

(7) The instruction to output is made requiring 3 microseconds.

(8) The output of the digital-to-analog converter is changed from the old value to the new value. The maximum possible time required for this process is 20 microseconds, but it was typically in the neighborhood of 1 microsecond.

(9) The output is held constant until the next command is issued.

As shown in figure 8, the total computer time involved between commanding a sample to be taken and commanding the calculated output is 212 microseconds; the actual time by which the output is delayed relative to the input is 200 microseconds. Thus, at a sampling frequency of 1000 samples per second (1000 μsec between samples), the computer is idle more than 78 percent of the time. At a sampling frequency of 100 samples per second, the idle time increases to almost 98 percent. Should it be desired to sample at a very high rate, 4000 samples per second can be handled, reducing idle time to less than 15 percent.

RESULTS AND DISCUSSION

Comparison of Analytical and Experimental Data

It was desired to have the various computer programs debugged before starting the wind tunnel testing. This was accomplished by simulating the inlet on an analog computer and then using the digital computer to control the inlet simulation. This simulation was based on linearized normal shock equations and one-dimensional wave equations for the subsonic duct. A description of this model and its simulation is found in reference 14.

Open-loop response. - Figure 9 shows the open-loop magnitude and phase response of P_{56} for the simulation and the experimental model, while the inlet was subjected to a downstream airflow disturbance. These responses as well as all the rest of the frequency response data presented have been normalized by the steady-state zero-to-peak

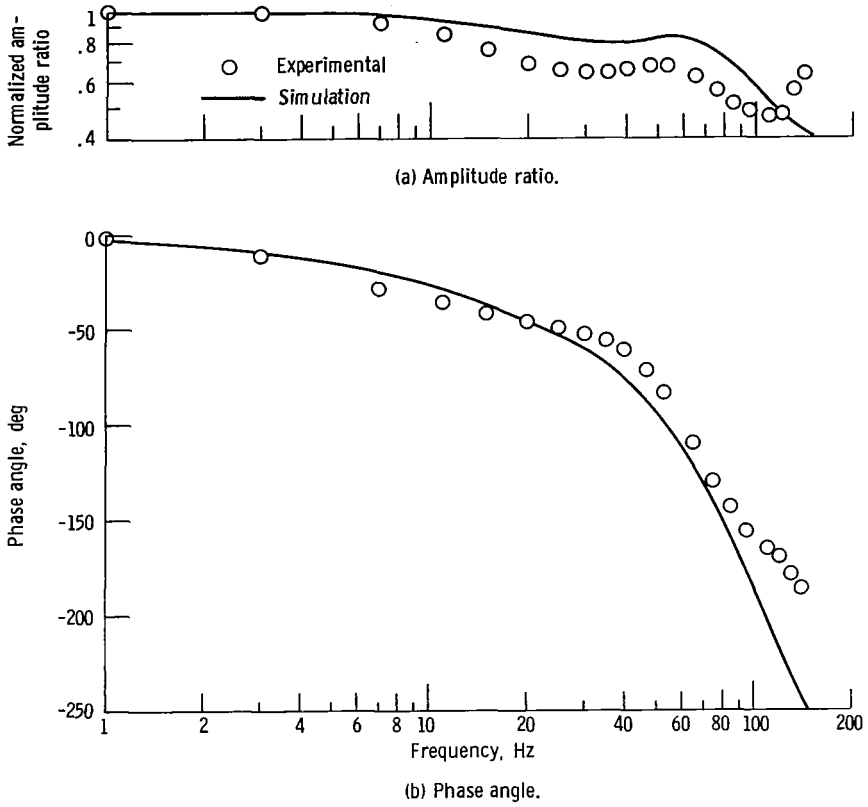

(a) Amplitude ratio.

(b) Phase angle.

Figure 9. - Comparison of simulation and experimental open-loop frequency responses of $\Delta P_{56}/\Delta W_{bt}$.

value. The magnitude and phase data agree fairly well out to about 100 hertz. The inlet simulation is somewhat conservative in that it shows slightly higher magnitudes and more phase lag than the experimental data did. Thus, the simulation should be adequate in determining what the experimental closed-loop frequency responses and controller gains should be for the various control algorithms.

Closed-loop responses. - Figures 10, 11, and 12 show a comparison of the closed-loop responses of the simulation and experimental inlet for the analog controller, for the digital z-transform controller, and for the digital backward difference equation controller, respectively. One thousand samples per second were used for the digital computer controllers. The responses of the inlet and its simulation agree fairly well out to about 100 hertz. This demonstrated the value of using the simulation for debugging the digital computer programs and for giving an approximate prediction of the form of the experimental responses. Actual comparisons between the analog and the various digital controls will be presented only for the experimental data and will be discussed next.

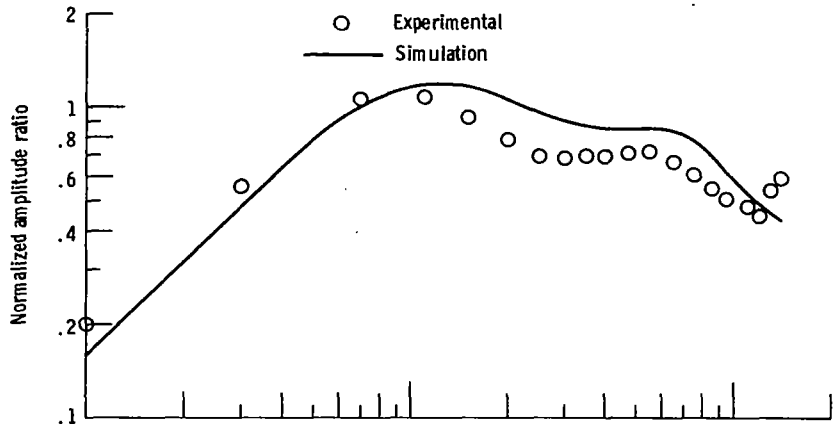

(a) Amplitude ratio.

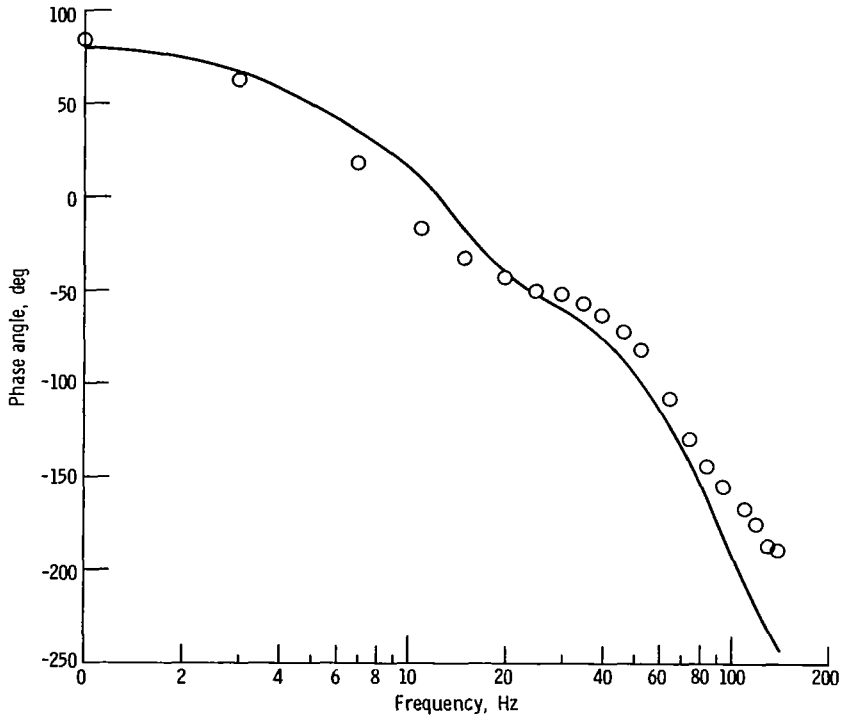

(b) Phase angle.

Figure 10. - Comparison of simulation and experimental closed-loop frequency responses of $\Delta P_{56}/\Delta W_{bd}$ using analog computer control.

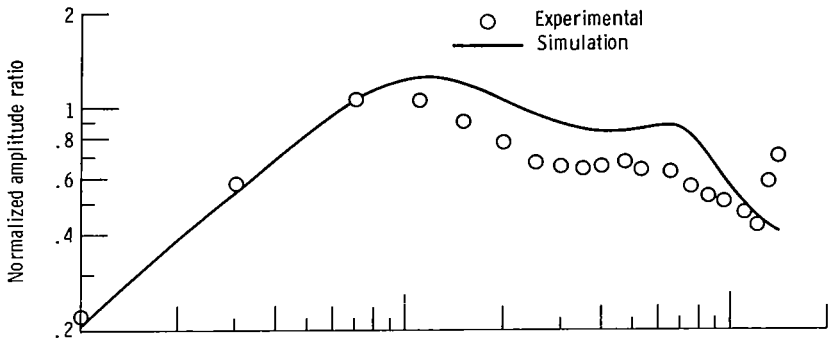

(a) Amplitude ratio

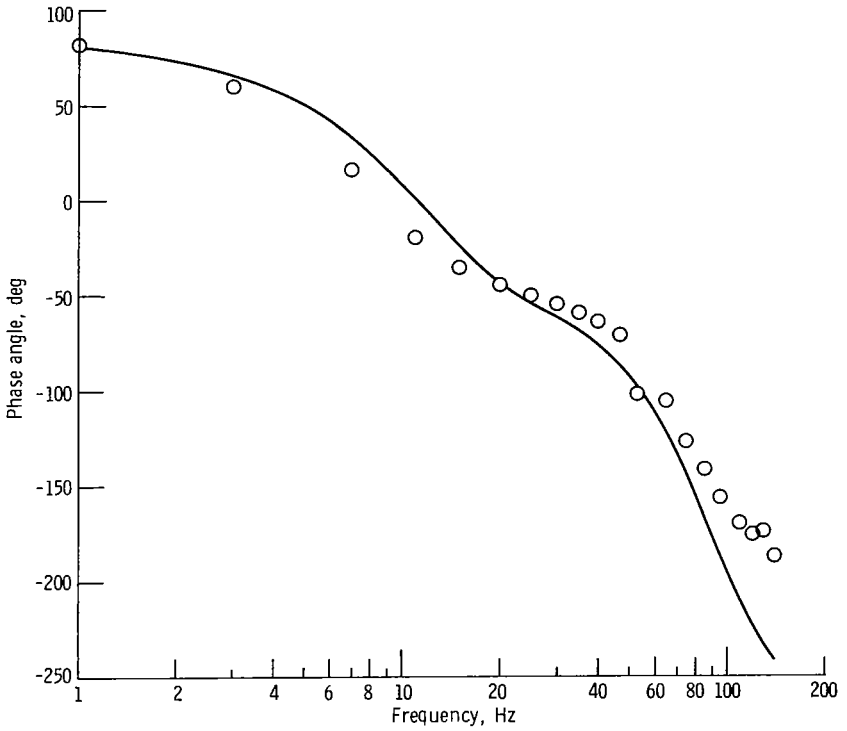

(b) Phase angle.

Figure 11. - Comparison of simulation and experimental closed-loop frequency responses of $\Delta P_{56}/\Delta W_{bd}$ using z-transform algorithm for digital computer control. Sample rate, 1000 samples per second.

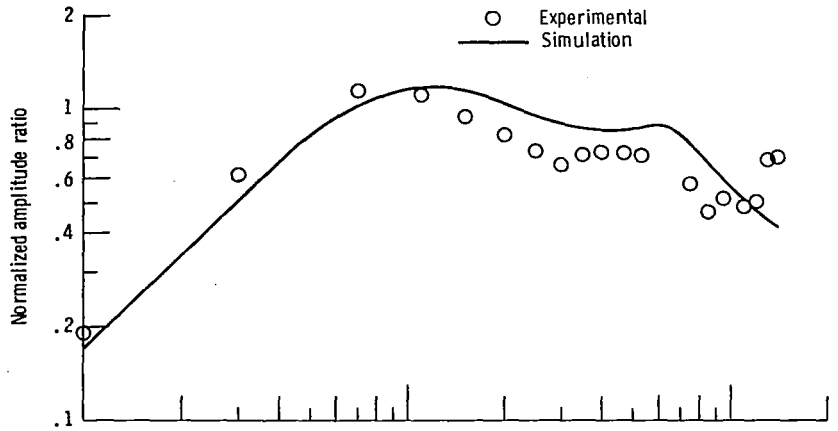

(a) Amplitude ratio.

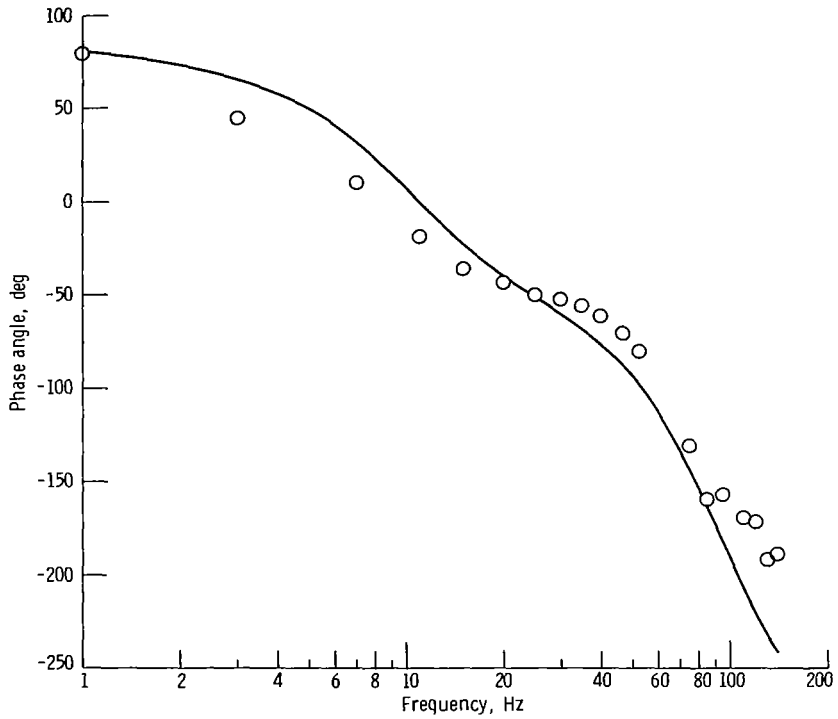

(b) Phase angle.

Figure 12. - Comparison of simulation and experimental closed-loop frequency responses of $\Delta P_{56}/\Delta W_{bd}$ using backward difference algorithm for digital computer control. Sample rate, 1000 samples per second.

Experimental Results for Evaluation of Digital Computer Normal Shock Control

Comparison of z-transform digital and analog computer control of normal shock position. - Baseline response using analog computer control: Figure 13 shows the experimental open-loop response (solid line) and three experimental closed-loop responses (various dashed lines) of P_{56} to a downstream airflow disturbance. The closed-loop-control responses representing different K_{c56}'s were obtained using an analog computer

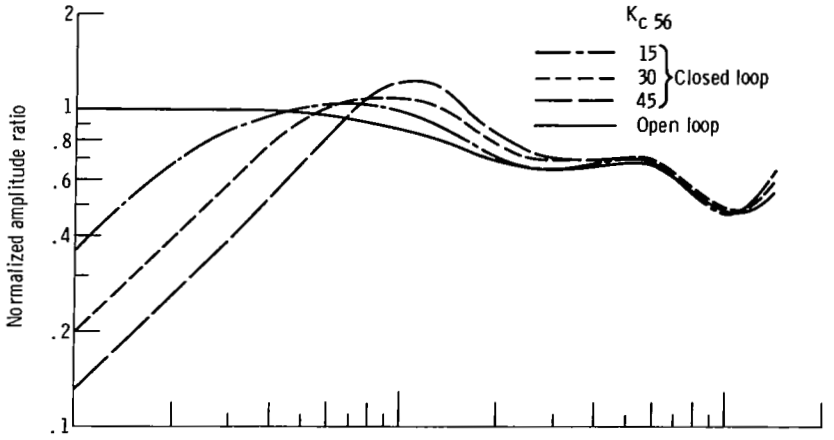

(a) Amplitude ratio.

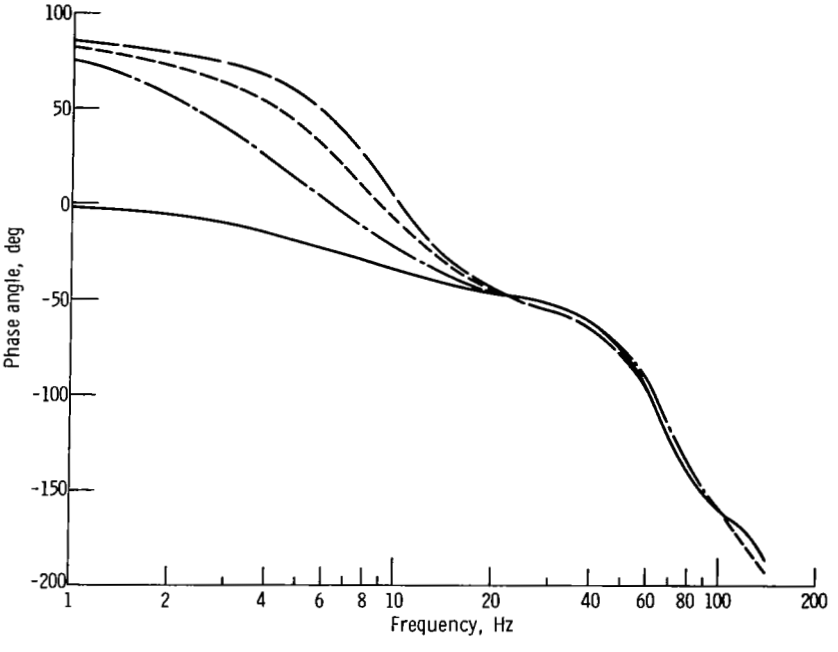

(b) Phase angle.

Figure 13. - Comparison of experimental open-loop and closed-loop $\Delta P_{56}/\Delta W_{bd}$ frequency responses using analog computer control and showing effects of varying controller gain.

to close the loop. The short-dashed curve is the closed-loop response for what will be called the nominal analog computer control gain ($K_{c56} = 30$). Except as noted all the other results shown in this report are for this value of K_{c56}. The long-dashed and dash-dotted curves are the closed-loop responses for K_{c56} equal to 45 and 15, respectively. The responses for different gains are given here to show the effect of gain on the nature of the closed-loop responses.

Response using z-transform digital computer control: Figure 14 shows a compar-

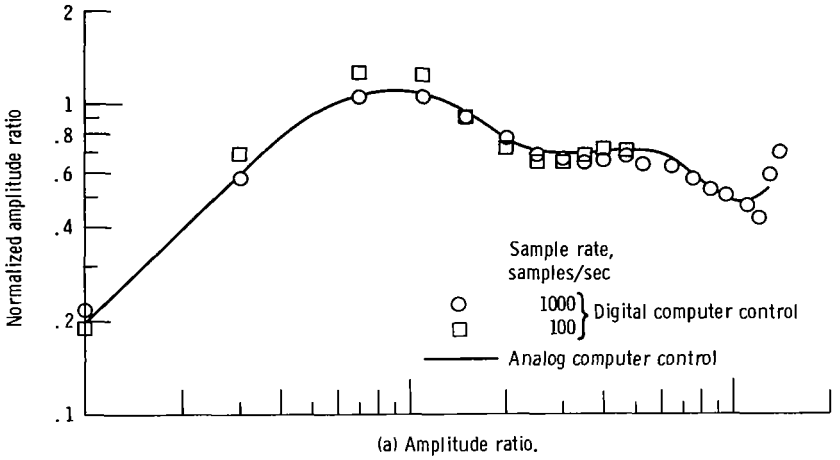

(a) Amplitude ratio.

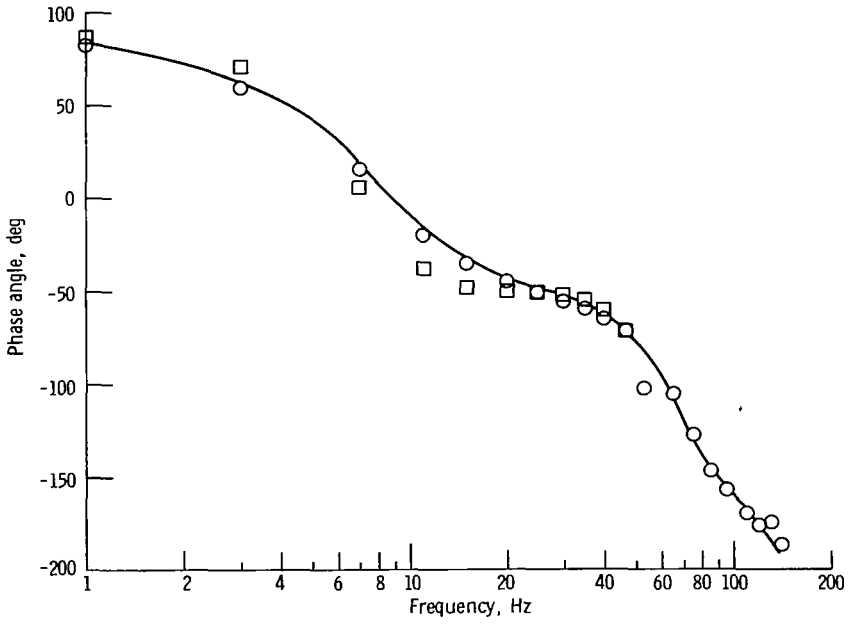

(b) Phase angle.

Figure 14. - Comparison of experimental closed-loop frequency responses of $\Delta P_{56}/\Delta W_{bd}$ using analog computer control and z-transform digital computer control at different sample rates.

ison of the closed-loop nominal control using the analog computer (dashed line) and the digital computer z-transform controller (circles and squares). The digital computer sampling rate for the closed-loop response shown by the circles and squares was 1000 samples per second and 100 samples per second, respectively. At 1000 samples per second (circles) the digital computer control essentially duplicated the analog computer control response including both magnitude and phase. The 100-sample-per-second (squares) data are slightly more resonant in the region of 9 hertz. These data are not plotted above a disturbance frequency of 50 hertz (half the sampling rate) because the responses became erratic due to a violation of the sampling theorem. This subject will be discussed more fully in the next section.

Since there is very little difference between the analog computer control response (continuous control) and the two z-transform digital computer control responses (discrete control) the assumption made in a previous section that the input and output samplers could be considered to be synchronous seems valid. Thus, for this system, the simpler control algorithm coefficients obtained by means of the z-transform seem adequate. It was not necessary to use the more complicated coefficients that would be obtained from the advanced z-transform method.

Minimum sampling rate limitations. - According to sampled-data theory, the sample rate must be at least twice as high as the highest frequency contained in the digital computer input data that significantly affects the system. The physical basis for this can be seen by studying figure 15. Figure 15(a) shows the system operating normally at a low disturbance frequency of 7 hertz. The disturbance bypass door (top trace) and P_{56} feedback signals (second trace) are sine waves at 7 hertz. The digital controller samples P_{56} at a rate of 100 times per second creating a stepwise command signal having 100 steps per second (third trace). The control bypass doors follow the command signal rounding the steps slightly (fourth trace) to control the input, thereby reducing the amplitude of the P_{56} excursion (relative to its open-loop value).

Figure 15(b) shows these same signals in the case of a disturbance frequency of 95 hertz. The problem is created by the fact that the discontinuous digital control samples the 95-hertz feedback signal 100 times a second. Therefore, it samples each successive sine wave at a slightly earlier point in its cycle. Each twentieth sample catches P_{56} at the same point. Thus the error signal experiences one complete cycle in 20 samples. This drives the control doors at 5 hertz. Thus the disturbance doors and control doors drive the system at 95 and 5 hertz, respectively. The P_{56} signal reflects these two inputs. At a sample rate of 1000 the problem did not occur. Thus, figure 15 demonstrates the importance of satisfying the sample theorem. References 12 and 13, in a discussion of general communication theory, show how the frequency spectrum of a sampled data signal can be distorted at low sampling rates.

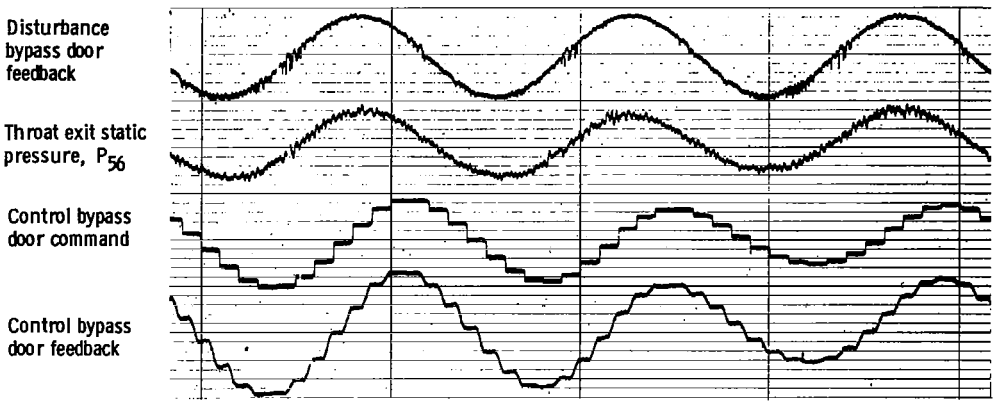

(a) 7-Hertz disturbance (no violation of sampling theorem).

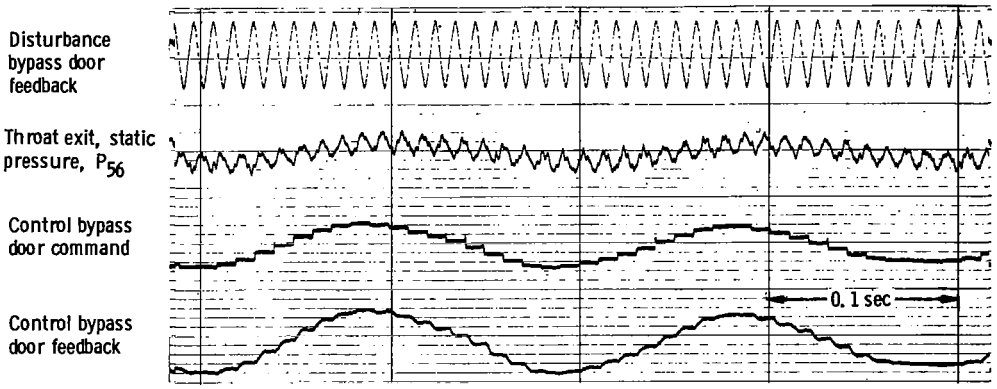

(b) 95-Hertz disturbance (violation of sampling theorem).

Figure 15. - Demonstration of violation of sample theoren using responses of closed-loop shock position digital computer control at disturbance frequencies of 7 and 95 hertz. Computer sample rate, 100 samples per second.

Comparison of digital computer control of normal shock position using z-transform and backward difference algorithms. - Figure 16 shows a comparison of the closed-loop responses using two different algorithms for the digital computer control. For these data 1000 samples per second were used. The solid line and circles indicates results for the z-transform and backward difference algorithms, respectively. These data agree well.

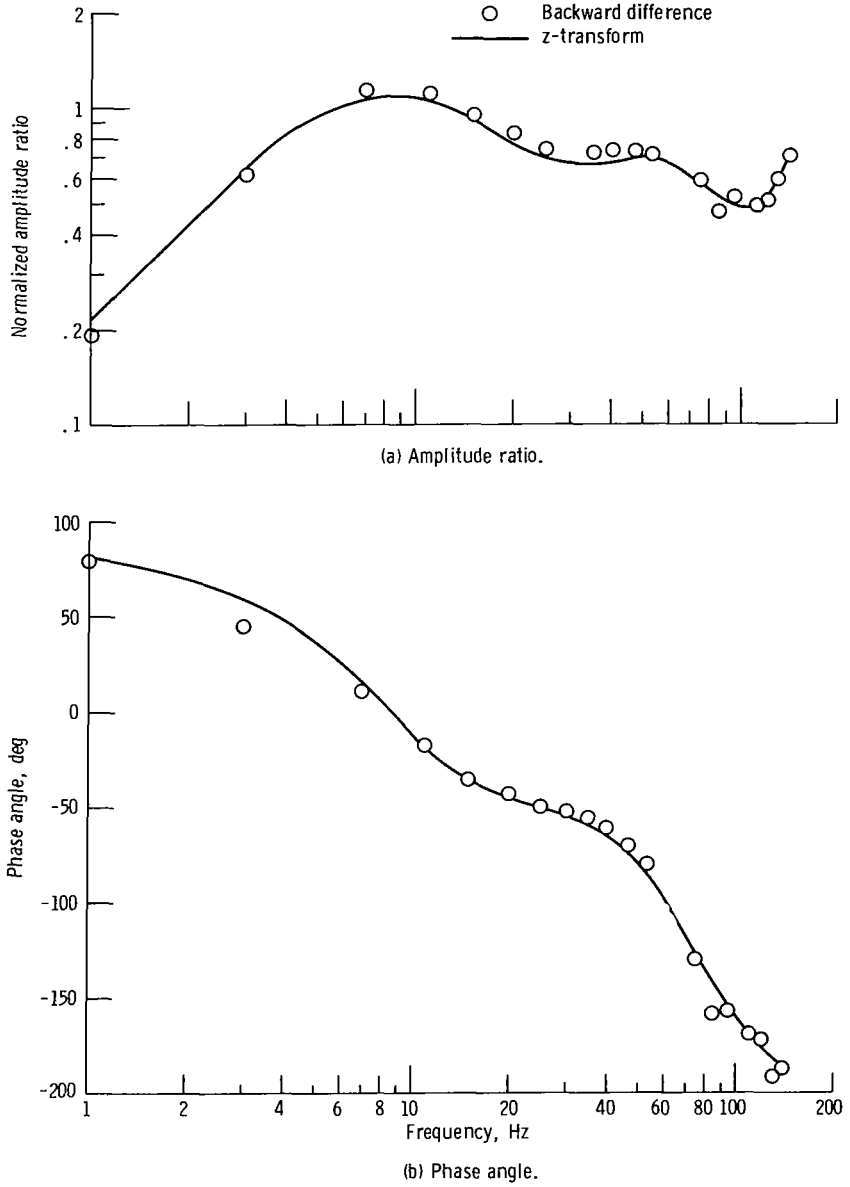

(a) Amplitude ratio.

(b) Phase angle.

Figure 16. - Comparison of experimental $\Delta P_{56}/\Delta W_{bd}$ closed-loop frequency responses for z-transform and backward difference digital computer algorithms using sample rate of 1000 samples per second.

Figure 17 shows a comparison of the closed-loop responses using the same two algorithms for the digital computer control but for a slower sample rate of 100 samples per second. Again the data were not plotted beyond 50 hertz because of the violation of sampling theory. These data are presented in order to show the effect of varying sample rate on the closed-loop digital computer control of shock position.

Comparing the data of figures 16 and 17 shows that the response using the z-transform method is slightly more resonant at the lower sample rate than at the higher sample rate. The response using the backward difference algorithm is essentially unchanged by varying the sample rate. Figures 16 and 17 indicate that, for this particular inlet, either computer algorithm would give essentially the same results.

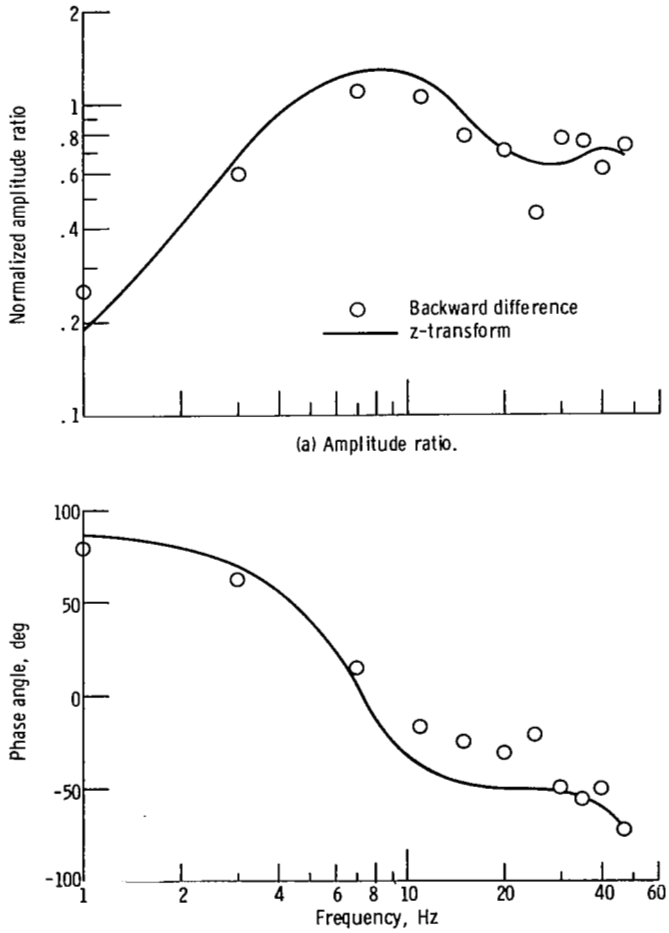

(a) Amplitude ratio.

(b) Phase angle.

Figure 17. - Comparison of experimental $\Delta P_{56}/\Delta W_{bd}$ closed-loop frequency responses for z-transform and backward difference digital computer algorithms using sample rate of 100 samples per second.

Normal shock position control using the electronic shock sensor for feedback. - All of the normal shock position controls tested were designed for using P_{56} as the feedback signal because it was decided to use a smooth continuous feedback signal in comparing analog and digital computer control. However, since a normal shock position sensing scheme did exist, even though it was a stepwise continuous signal, it was decided to try to use this signal for the feedback signal for the normal shock position controllers. This would be a better signal to use for future control testing because shock position is the ac-

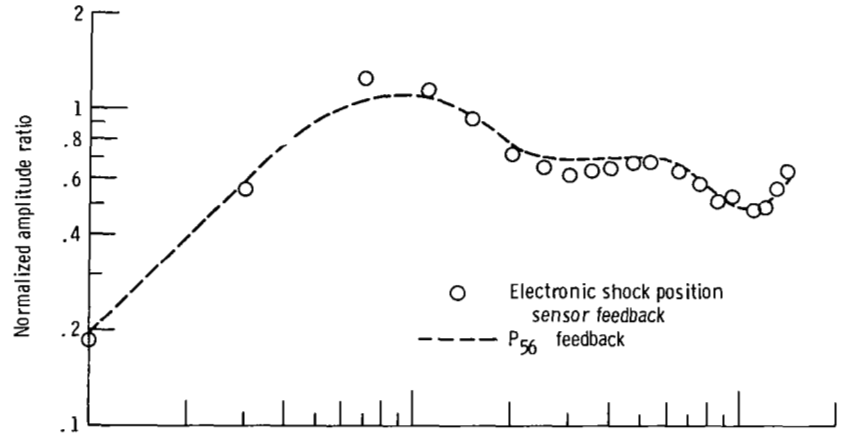

(a) Amplitude ratio.

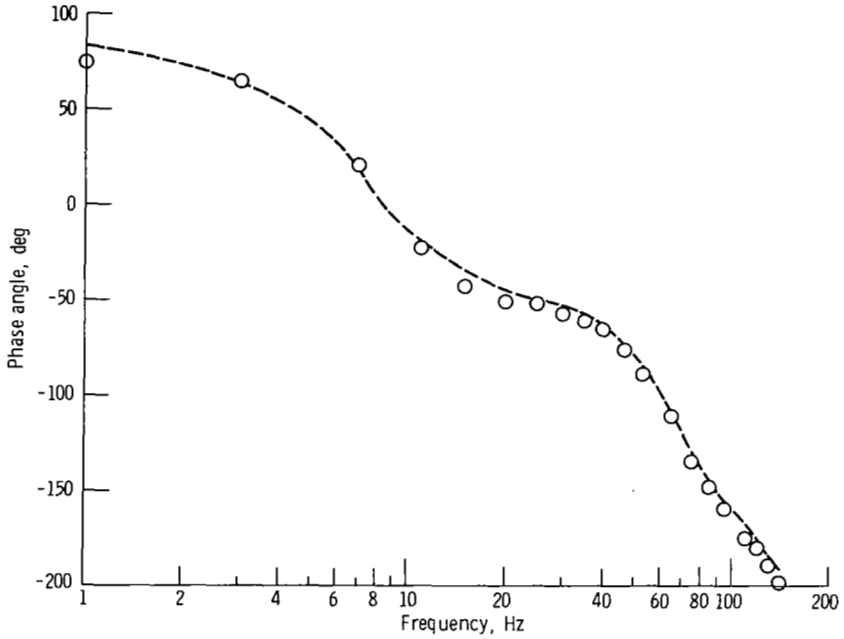

(b) Phase angle.

Figure 18. - Comparison of experimental $\Delta P_{56}/\Delta W_{bd}$ closed-loop frequency responses for analog computer control using either P_{56} or electronic shock position sensor output as feedback signal (controller gain adjusted to give same loop gain).

tual variable to be controlled. It was decided to merely substitute the shock position signal for the P_{56} feedback signal without modifying the controller dynamics. The controller gain was then adjusted until the loop gain was the same for both kinds of feedback signals. A discussion of the shock position criterion and its implementation is given in appendix B.

Figure 18 shows a comparison for the analog computer normal shock position control using either P_{56} or the electronic shock position sensor output as the feedback signal.

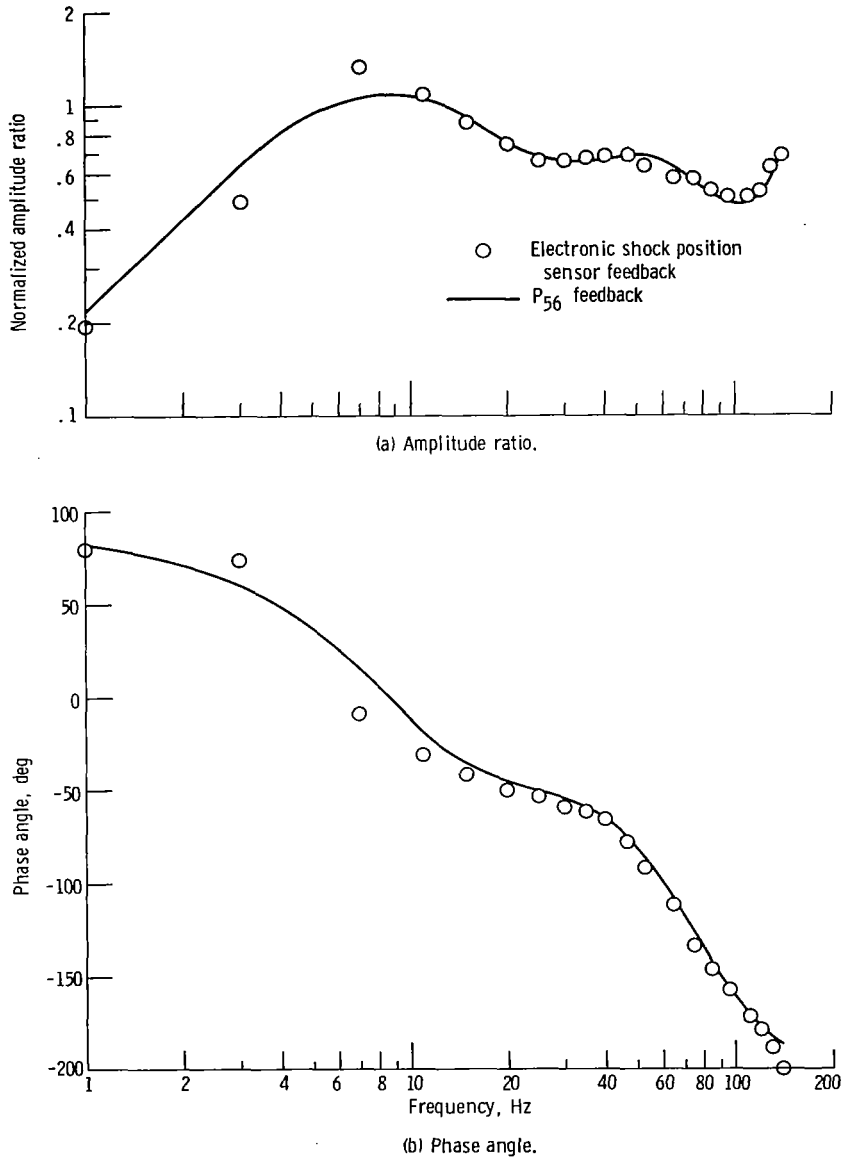

Figure 19. - Comparison of experimental $\Delta P_{56}/\Delta W_{bd}$ closed-loop frequency responses for z-transform digital computer control using either P_{56} or electronic shock position sensor output as feedback signal (controller gain adjusted to give same loop gain)

Figure 19 shows a comparison for the z-transform normal shock position control using either P_{56} or the electronic shock position sensor as feedback signals. These figures show that normal shock position control as indicated by P_{56} is almost identical for both types of feedback signals. The digital computer control (fig. 19) using the shock position sensor as the feedback signal is more resonant in the region of 7 hertz than the control using P_{56} as the feedback signal. But the difference is minor and might not exist if the controller dynamics were slightly modified for the control using the shock sensor as the feedback signal.

Experimental Results for Evaluation of Digital Computer Restart Control

Besides control of normal shock position, an inlet control for a mixed-compression inlet must be capable of restarting the inlet and bringing it back to its operating point when an inlet unstart occurs. An analog computer control was previously developed for this application and reported in reference 4. It was setup again in the present investigation for use as a standard of comparison. The same restart controller was programmed on the digital computer using the previously discussed z-transform normal shock position control during the unstart-restart transient. The digital computer restart control was tested using sample rates of 1000 and 100 samples per second.

Figure 20 shows the restart control system schematic. In each case P_{cl}, H_{th}, P_{56}, and centerbody position were measured and fed into the computer. The computer performed the appropriate calculations and then sent commands to the bypass door and centerbody servos.

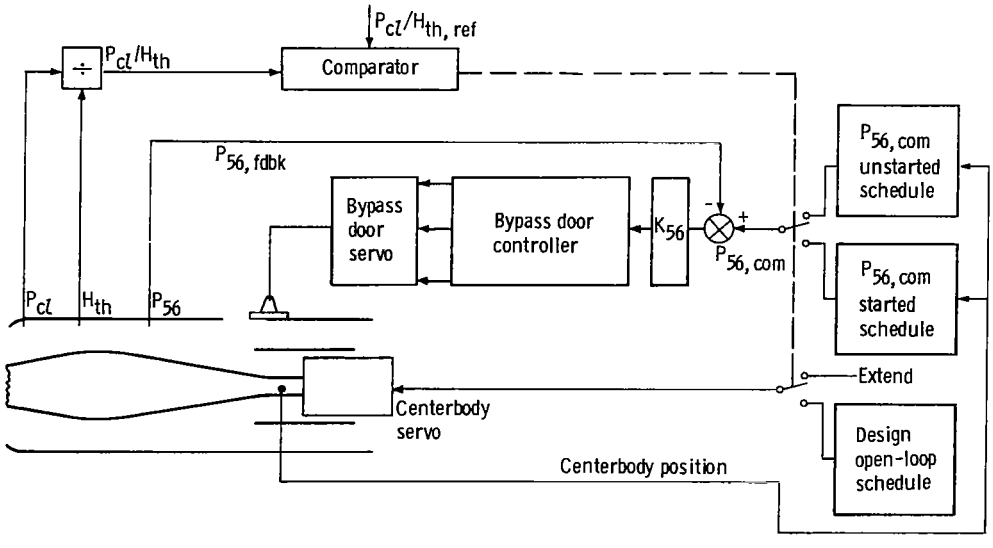

Figure 20. - Restart control system schematic.

A ratio of a cowl lip static pressure P_{cl} to a throat total pressure H_{th} was compared to a reference value to determine if the inlet was started or unstarted. When the inlet was started, the value of the ratio was below the reference value. When the inlet unstarted, the value of the ratio exceeded the reference value and the comparator switched to the unstarted control mode. This comparator selected the command signals being sent to the centerbody and bypass door servos. When an unstart was detected, the comparator switched the centerbody position command signal from its design operating point position to an extended position. At the same time the unstart comparator switched, the P_{56} command from its started schedule to its unstarted schedule. The centerbody extended, increasing the ratio of throat-to-capture flow area, until the inlet restarted. Once the inlet restarted, the comparator switched the servocommand signals back to their started schedules. The centerbody retracted to its design value and the inlet pressure was gradually increased to its original operating point value as the centerbody retracted. Each of the P_{56} command schedules was a stepwise continuous function of centerbody position. For any given centerbody position higher pressures can be obtained when the inlet is started as compared to when the inlet is unstarted.

Figure 21 shows an unstart-restart transient for the analog computer version of the restart control. This transient is presented as a reference for comparison and evaluation of the digital computer version of the restart control. A detailed discussion of the unstart-restart transient will be made here.

When the transients are presented for the digital computer version of the restart control, only the differences between the traces for the analog and digital computer restart controls will be discussed. The base line of the arrow on the left of each trace is the zero for that trace. The direction of the arrows indicates the direction of increasing value. The following sequence describes the various events that occurred during the unstart-restart transient.

(1) The normal shock was positioned close to the throat as evidenced by the high level of P_{56}.

(2) The three disturbance doors were pulsed closed in order to unstart the inlet.

(3) The control bypass doors started to open to compensate for the disturbance but they could not move fast enough and the inlet unstarted. Then they started to close, reacting to the decreased P_{56} signal, until the unstart comparitor switched the P_{56} command (item 8).

(4) When the inlet unstarted, the pressure recovery H_{cf}/H_0 took a sudden large drop thereby decreasing inlet performance.

(5) The inlet unstart is also evidenced by the sudden large drop in P_{56}.

(6) The unstart signal exceeded the reference value indicating the inlet has unstarted.

(7) The centerbody was commanded to move to an extended position that would allow the inlet to restart.

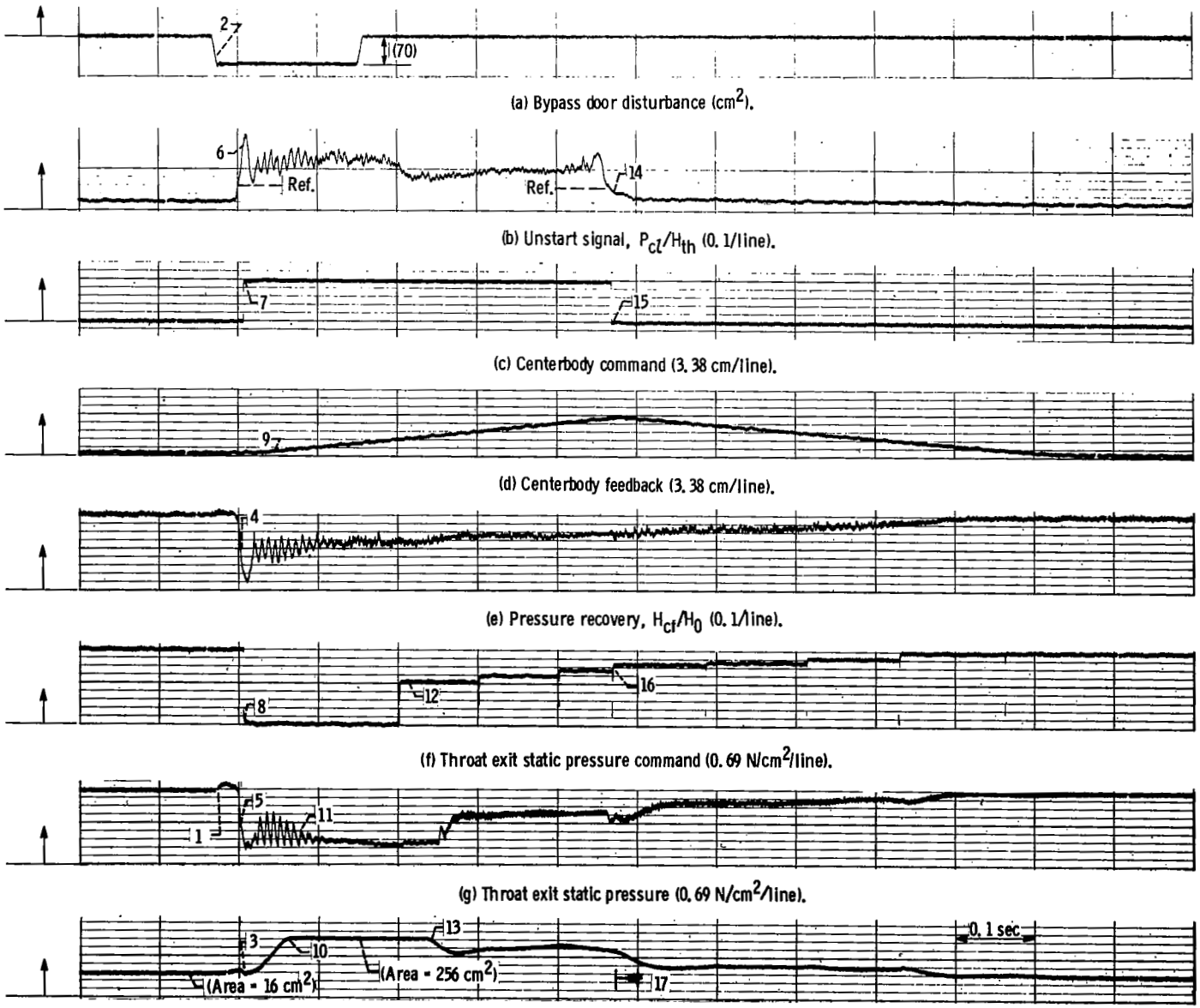

(a) Bypass door disturbance (cm^2).

(b) Unstart signal, P_{cI}/H_{th} (0.1/line).

(c) Centerbody command (3.38 cm/line).

(d) Centerbody feedback (3.38 cm/line).

(e) Pressure recovery, H_{cf}/H_0 (0.1/line).

(f) Throat exit static pressure command (0.69 N/cm^2/line).

(g) Throat exit static pressure (0.69 N/cm^2/line).

(h) Control bypass door feedback (1.0 V/line).

Figure 21. - Unstart-restart transient for analog computer restart control.

(8) The command to the P_{56} pressure control was switched from the started to the unstarted schedule (6.21 to 0 N/cm^2). This was done in order to quickly open the control bypass doors and thus stabilize the inlet.

(9) The centerbody began to extend in order to restart the inlet.

(10) The control bypass doors opened in response to the change in P_{56} command (item 8).

(11) The inlet stabilized as evidenced by the decreased pressure oscillations in P_{56}.

(12) As the centerbody extended, higher levels in P_{56} were commanded.

(13) The control bypass doors began to close when it is possible to obtain increased inlet pressures as evidenced by the increase in P_{56}.

(14) The inlet restarted as indicated when the unstart signal dropped below the reference value.

(15) The centerbody was commanded to return to its design position.

(16) The command to the bypass door control switched to the started schedule.

(17) The control bypass doors continued to close responding to increasingly higher P_{56} commands, thus increasing inlet pressure recovery until the inlet returned to its operating point condition. The unstart-restart transient was completed in just a little more than 1 second.

Figure 22 shows an unstart-restart transient for the digital computer version of the restart control. The normal shock position control used the z-transform algorithm, and it was the same one that was discussed previously in figure 14. For this test the sample rate was 1000 samples per second. It should be noted that for figures 22 and 23 a trace of the control bypass door command signal was included between the traces of the bypass door feedback signal and the P_{56} signal.

A comparison of figures 21 and 22 indicates that the two responses are essentially the same except for the initial response of the control bypass doors. This difference is a result of the specific hardware used. In the case of the digital control (fig. 22) a priority interrupt requiring only 10 microseconds was all that was needed to tell the control the inlet was unstarted. In the case of the analog control (fig. 21) a relay switch requiring 5 milliseconds to switch was used to tell the control that the inlet was unstarted. The result was that for the analog control the P_{56} command signal did not switch to a lower unstarted value as fast as that for the digital control. Because of this, the control bypass doors (for the analog restart control) started to close in order to maintain the higher commanded pressure. For this particular inlet it would be desirable to use unstart comparators faster than 5 milliseconds so that the doors do not first close before opening to stabilize the inlet when it unstarts. This is because it is desirable to open the bypass doors as soon as possible after the inlet unstarts to avoid an unstable buzz condition.

Figure 23 shows the unstart-restart transient using the same digital computer control just discussed except for this test the sample rate was decreased to 100 samples per

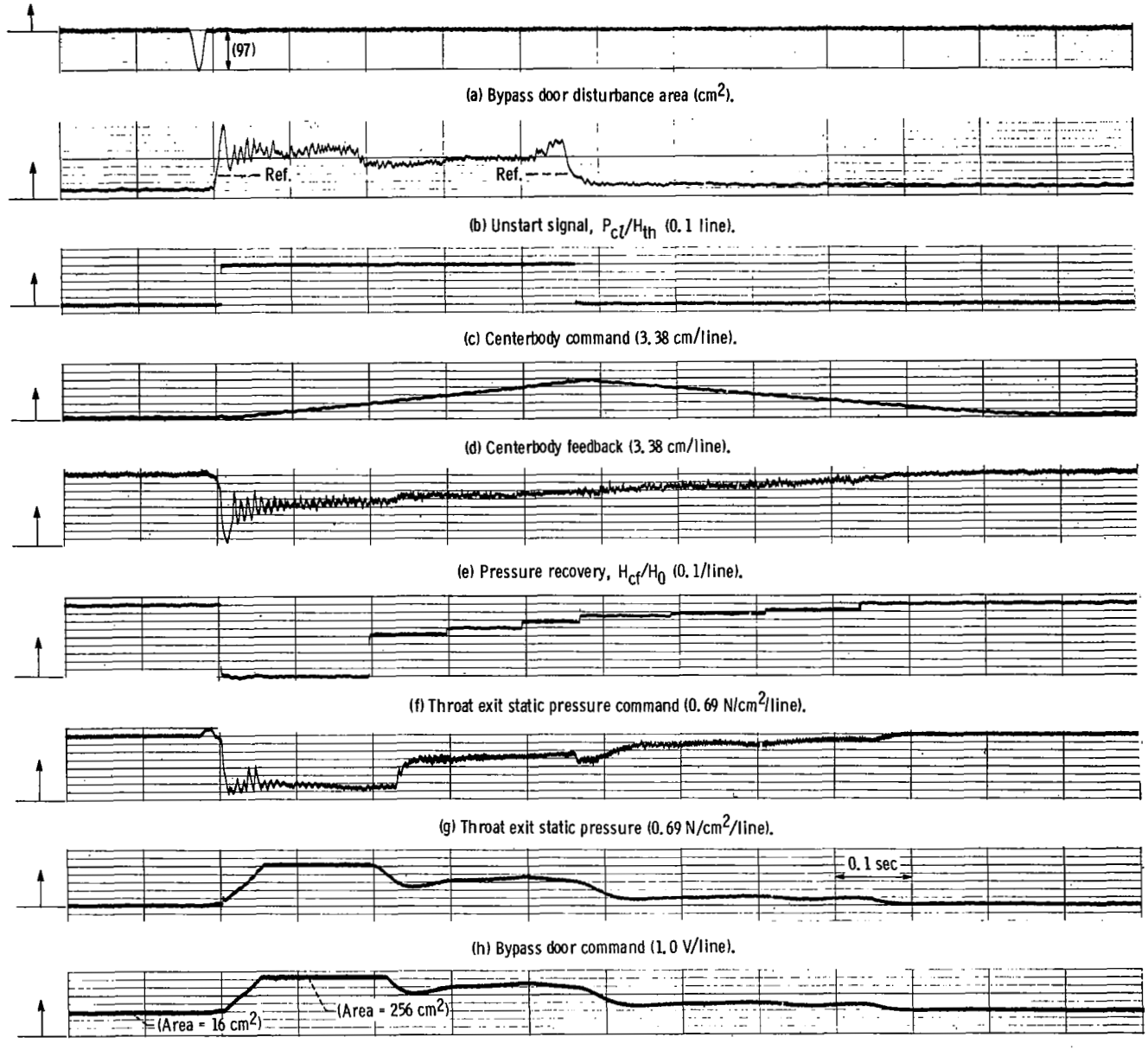

(a) Bypass door disturbance area (cm^2).

(b) Unstart signal, P_{cl}/H_{th} (0.1 line).

(c) Centerbody command (3.38 cm/line).

(d) Centerbody feedback (3.38 cm/line).

(e) Pressure recovery, H_{cf}/H_0 (0.1/line).

(f) Throat exit static pressure command (0.69 N/cm^2/line).

(g) Throat exit static pressure (0.69 N/cm^2/line).

(h) Bypass door command (1.0 V/line).

(i) Control bypass door feedback (1.0 V/line).

Figure 22. - Unstart-restart transient for z-transform digital computer restart control using sample rate of 1000 samples per second.

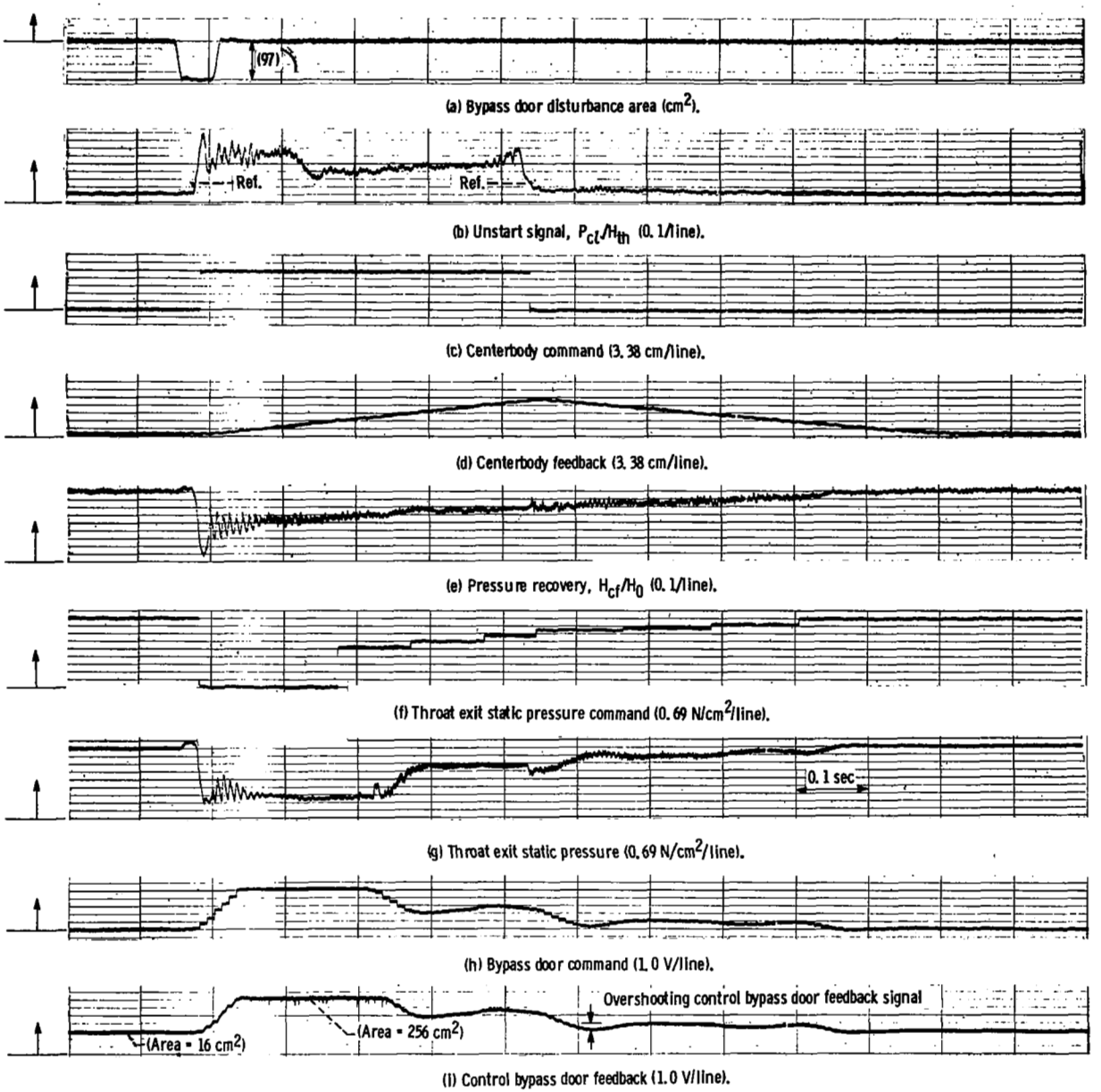

(a) Bypass door disturbance area (cm^2).

(b) Unstart signal, P_{cf}/H_{th} (0.1/line).

(c) Centerbody command (3.38 cm/line).

(d) Centerbody feedback (3.38 cm/line).

(e) Pressure recovery, H_{cf}/H_0 (0.1/line).

(f) Throat exit static pressure command (0.69 N/cm^2/line).

(g) Throat exit static pressure (0.69 N/cm^2/line).

(h) Bypass door command (1.0 V/line).

(i) Control bypass door feedback (1.0 V/line).

Figure 23. - Unstart-restart transient for z-transform digital computer restart control using sample rate of 100 samples per second.

second. The discrete nature of the digital controller is evident in the control bypass door command signal. At this lower sample rate, the normal shock position control becomes less stable. This is shown by the overshooting in the control bypass door feedback signal as pointed out in figure 23.

SUMMARY OF RESULTS

A modern digital computer process controller was used to successfully control a Mach 2.5 axisymmetric mixed-compression inlet against downstream airflow disturbances. Two controls were programmed on the digital computer. One was a normal shock position control and the other was an inlet restart control. Using digital computer sample rates of 1000 samples per second, the digital normal shock position and restart controls essentially duplicated the results of controlling the inlet with an analog computer. However, the problems of digital control such as using adequate sampling rates and stable computer algorithms could not be ignored.

The following items were also demonstrated:

1. The value of using an analog computer inlet simulation to debug the digital computer control algorithms and to predict the nature of open- and closed-loop normal shock position dynamics.

2. Digital computer algorithms derived by using either the z-transform or a finite difference method could be used successfully for controlling normal shock position.

3. Violations of the sampling theorem adversely effects the response of the closed-loop system.

4. An electronic shock position sensor having a stepwise continuous output signal proportional to shock position can be substituted for the throat exit static pressure feedback for both the analog computer and z-transform digital computer controls. The frequency responses were shown to be nearly identical regardless of which signal was used.

5. The inlet restart control using the z-transform digital computer algorithm for normal shock position control at a sample rate of 100 samples per second gave an adequate restart transient response. It was slightly less stable than the control using a sample rate of 1000 samples per second.

Lewis Research Center,
National Aeronautics and Space Administration,
Cleveland, Ohio, April 5, 1972,
764-74.

APPENDIX A

SYMBOLS

$a, b, \ldots, h$	static pressure taps on inlet cowl surface (also refers to pressures measured at those taps)
BPC	bypass door command
$C_1, C_2, \ldots, C_5$	constant coefficients
$E_1, E_2, \ldots, E_5$	percent error in algorithm coefficients relative to advanced z-transform coefficients
ERR	error term
G_{bc}	transfer function between the bypass door command voltage and the control bypass door airflow, kg/sec/V
G_c	controller transfer function, V/V
G_I	transfer function between disturbance bypass door airflow and inlet throat exit static pressure, $N/cm^2/kg/sec$
G_o	transfer function for a zero order hold
G_{sp}	transfer function between throat exit static pressure and shock position, $cm/N/cm^2$
H	total pressure, N/cm^2
K_{c56}	compensator gain for controller using P_{56} for feedback, V/V
M	Mach number
n	integers (1, 2, 3, etc.)
P	static pressure, N/cm^2
P_{56}	throat exit static pressure, N/cm^2
R_c	cowl lip radius, cm
s	Laplace variable, 1/sec
T	sample period, sec
W	airflow, kg/sec
X	distance from the cowl lip, cm
x_{sp}	shock position, cm
y	general term representing any particular variable

z	z-transform variable
$\mathscr{Z}$	denotes z-transform operation
Δ	indicates small change in particular variable
δ	computation time/sample period
ρ	damping ratio
ω_1, ω_2	frequency, rad/sec

Subscripts:

a	advanced
bc	control bypass doors
bd	disturbance bypass doors
bt	total bypass doors
c	control
$c\ell$	cowl lip
cf	compressor face
com	command
fdbk	feedback
ref	reference
th	throat
0	free stream

APPENDIX B

SHOCK POSITION SENSOR

During the test program, the throat exit static pressure P_{56} was used as the means of evaluating control performance and was usually used as the normal shock control feedback variable. A more direct measurement of normal shock position was desired to evaluate the possibility of using shock position as the control feedback variable and to provide a control room display of shock position. In an attempt to satisfy these requirements a shock position sensing scheme with an electronic output was devised and used.

Shock Position Criterion

A common way to determine shock position is to observe the static pressure profile in the vicinity of the shock. For inlets with internal compression the ideal pressure profile occurs as shown in figure 24. The minimum supersonic flow Mach number occurs at the inlet throat. Downstream of the throat, the Mach number increases and static pressure decreases as area increases. At the normal shock there is a discontinuous rise in pressure. Downstream of the shock, the pressure continues to rise since the flow is subsonic and area continues to increase.

In a real inlet, the pressure profile can be measured by a series of closely spaced static pressure taps. That was done in this program by connecting dynamic pressure transducers to the eight static pressure taps (a to h) shown in figure 4. Figure 25 shows typical pressure profiles that were measured for eight different shock positions. Each

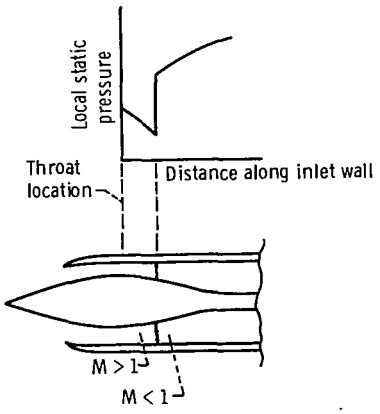

Figure 24. - Ideal static pressure profile in vicinity of normal shock.

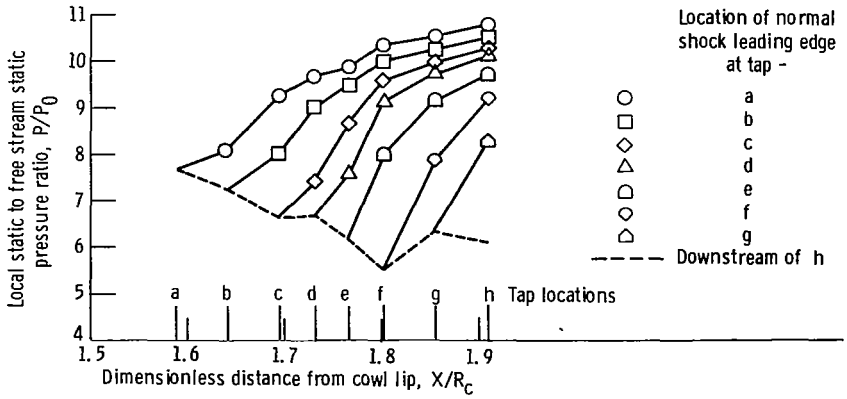

Figure 25. - Typical inlet cowl static pressure profiles in vicinity of normal shock. Free stream Mach number, 2.5; angle of attack, 0^{o}.

profile was obtained with the leading edge of the shock just downstream of a tap as noted on the figure. Each profile upstream of the shock's leading edge coincides with the dashed line. The nonideal nature of the profiles is due to such things as shock-boundary layer interaction, oblique shock reflections, and a finite shock train thickness. Although the pressure rise across the shock is not discontinuous as in the ideal case, there is a rather large pressure gradient in the vicinity of the shock.

The criterion for determining shock position, which was based on profiles such as those of figure 25, was to find the first tap having a pressure higher than that of tap a. The shock would then be said to be located between that tap and the tap just upstream of it. For example, from the profile with the symbol ⌂ the shock would be determined to be between taps e and f (where tap f is the first tap with a pressure higher than tap a and tap e is the adjacent upstream tap). The resolution of this scheme is, of course, limited to the spacing of the taps. Also, when the shock is outside of the tap region, the only indication is whether the shock is upstream of b or downstream of h. It can also be noted from figure 25 that, for two of the profiles (diamonds and triangles), the shock would be determined to be one tap aft of the actual position. These were not considered to be serious steady-state errors.

Shock Sensor Implementation

The shock sensor was implemented using electronic comparators and analog summing amplifiers. The sensor logic is shown schematically in figure 26. The transducer

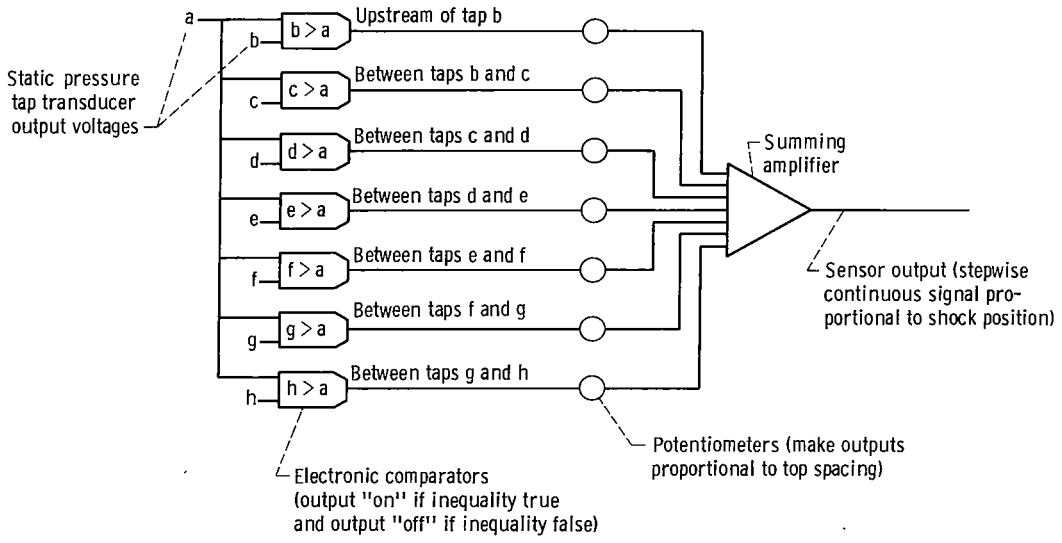

Figure 26. - Analog implementation of electronic normal shock position sensor.

signals representing pressures at taps b to h were compared to the transducer signal representing the pressure at tap a by means of electronic comparators. Each comparator had a voltage output corresponding to an "on" or "off" state depending on whether the pressure at tap a was less or greater respectively, than the pressure it was being compared with. A steady-state voltage change equivalent to 0.03 newton per square centimeter was required to switch the comparator from one state to the other. A step change in voltage equivalent to 0.14 newton per square centimeter resulted in a comparator switching time of about 0.3 millisecond. The outputs of the comparators were weighted according to tap spacing by means of potentiometers and were then summed. The resultant sensor output was an electronic stepwise continuous signal proportional to shock position. The individual comparator outputs were used to turn on lights in the wind tunnel control room for a visual display of shock position.

The shock position criterion logic was also programmed on the digital computer. In this case the signals representing the tap pressures were fed to the digital computer through an analog to digital converter. First, the signal from the pressure transducer at tap a was sampled by the computer. Then the signal at tap b was sampled and compared to that at tap a and so on until the shock was located. About 50 microseconds was required to sample a tap pressure and compare it to the pressure at tap a. Shock position was calculated once during each update period. This loss of computing time could be avoided by doing the comparison of signals with analog electronics as shown in figure 26 and feeding one stepwise-continuous shock position signal into the digital system. The digital control results shown in this report, however, were obtained by the all digital method of shock sensing.

REFERENCES

1. Neiner, George H.; Crosby, Michael J.; and Cole, Gary L.: Experimental and Analytical Investigation of Fast Normal Shock Position Controls for a Mach 2.5 Mixed Compression Inlet. NASA TN D-6382, 1971.

2. Cole, Gary L.; Neiner, George H.; and Wallhagen, Robert E.: Coupled Supersonic Inlet-Engine Control Using Overboard Bypass Doors and Engine Speed to Control Normal Shock Position. NASA TN D-6019, 1970.

3. Paulovich, Francis J.; Neiner, George H.; and Hagedorn, Ralph E.: A Supersonic Inlet-Engine Control Using Engine Speed as a Primary Variable for Controlling Normal Shock Position. NASA TN D-6021, 1971.

4. Cole, Gary L.; Neiner, George H.; and Crosby, Michael J.: An Automatic Restart Control System for an Axisymmetric Mixed-Compression Inlet. NASA TN D-5590, 1969.

5. Chun, K. S.; and Burr, R. H.: A Control System Concept for an Axisymmetric Supersonic Inlet. J. Aircraft, vol. 6, no. 4, July-Aug. 1969, pp. 306-311.

6. Schweikhardt, R. G.; and Grippe, R. P.: Investigations in the Design and Development of a Bypass Door Control System for an SST Axisymmetric Intake Operating in the External Compression Mode. Paper 70-695, AIAA, June 1970.

7. Cubbison, Robert W.; Meleason, Edward T.; and Johnson, David F.: Effect of Porous Bleed in a High-Performance Axisymmetric, Mixed-Compression Inlet at Mach 2.50. NASA TM X-1692, 1968.

8. Cubbison, Robert W.; Meleason, Edward T.; and Johnson, David F.: Performance Characteristics from Mach 2.58 to 1.98 of an Axisymmetric Mixed-Compression Inlet System with 60-Percent Internal Contraction. NASA TM X-1739, 1969.

9. Wasserbauer, Joseph F.: Dynamic Response of a Mach 2.5 Axisymmetric Inlet with Engine or Cold Pipe and Utilizing 60 Percent Supersonic Internal Area Contraction. NASA TN D-5338, 1969.

10. Neiner, George H.: Servosystem Design of a High-Response Slotted-Plate Overboard Bypass Valve for a Supersonic Inlet. NASA TN D-6081, 1970.

11. Arpasi, Dale J.; Zeller, John R.; and Batterton, Peter G.: A General Purpose Digital System for On-Line Control of Airbreathing Propulsion Systems. NASA TM X-2168, 1971.

12. Kuo, Benjamin C.: Analysis and Synthesis of Sampled-Data Control Systems. Prentice Hall, Inc., 1963.

13. Tou, Julius T.: Digital and Sampled-Data Control Systems. McGraw-Hill Book Co., Inc., 1959.

14. Willoh, Ross G.: A Mathematical Analysis of Supersonic Inlet Dynamics. NASA TN D-4969, 1968.

NASA-Langley, 1972 —— 28 E-6498